THE AUTOMATED GEOSPATIAL WATERSHED ASSESSMENT TOOL (AGWA): USING RAINFALL AND STREAMFLOW RECORDS FROM BURNED WATERSHEDS TO EVALUATE AND IMPROVE PARAMETER ESTIMATIONS

by

Brian Scott Sheppard

A Thesis Submitted to the Faculty of the

DEPARTMENT OF HYDROLOGY AND WATER RESOURCES

In Partial Fulfillment of the Requirements
For the Degree of

MASTER OF SCIENCE

WITH A MAJOR IN HYDROLOGY

In the Graduate College

THE UNIVERSITY OF ARIZONA

2016

STATEMENT BY AUTHOR

This thesis titled The Automated Geospatial Watershed Assessment Tool (AGWA): Using Rainfall and Streamflow Records from Burned Watersheds to Evaluate and Improve Parameter Estimations prepared by Brian Scott Sheppard has been submitted in partial fulfillment of requirements for a master's degree at the University of Arizona and is deposited in the University Library to be made available to borrowers under rules of the Library.

SIGNED: Brian Scott Sheppard

APPROVAL BY THESIS DIRECTOR

This thesis has been approved on the date shown below:

_____ ___4/29/2016_____

Thomas Meixner Date

Professor of Hydrology

ACKNOWLEDGEMENTS

This research was made possible through funding provided by the Bureau of Land Management and the Department of Interior Burned Area Emergency Response Program. Special thanks are given to T.J. Clifford, Phil Guertin and Dave Goodrich for guidance and facilitation of this thesis.

Remote sensing work for this research was done in collaboration with Mark Kautz, a School of Natural Resources and the Environment master's student.

TABLE OF CONTENTS

LIST OF FIGURES

LIST OF TABLES

ABSTRACT

Precipitation and runoff records from several burned watersheds have been used to evaluate the performance of the Automated Geospatial Watershed Assessment (AGWA) tool as it is used to assign parameters to the KINmatic runoff and EROSion Model 2 (KINEROS2). This modeling scheme is used by the Department of Interior Burned Area Emergency Response (DOI BAER) teams to assess flooding and erosion risk immediately following a wildfire. Although DOI BAER teams use this parameterization/modeling framework to assess the relative change in watershed behavior following a wildfire by driving the model with National Oceanic and Atmospheric Administration (NOAA) design storms, calibrations performed on actual events using rainfall estimations provided by rain gages and radar to drive the model provides insight into the model's performance, and potentially informs changes and developments to the AGWA parameter estimation scheme. Results indicate that current parameter modifications made by AGWA to represent fire impacts provide reasonable results for DOI BAER relative change risk assessments, though additional modifications to saturated hydraulic conductivity may be necessary to represent a broader range of storm intensity.

1. INTRODUCTION

Runoff response to rainfall changes following a wildfire (DeBano et al., 1998). This is a result of the burning of canopy cover and organic litter (duff), which decreases interception and surface roughness, respectively. Hydrophobic soils also can form as a result of wildfire (DeBano et al., 1998), which can further reduce infiltration rates. The loss of interception, decrease in surface roughness and decrease in infiltration rates all contribute to an increase in surface runoff. Figure 1 illustrates the difference in storm response for unburned and burned conditions. The most notable differences in response to similar sized storms at the same watershed (Marshall Gulch, Figure 1) is that the peak flow rates for the post-fire flow is 25 times greater than the pre-fire flow, and the duration of the pre-fire storm flow is much longer, spanning 10 days as opposed to several hours. This dramatic increase in peak runoff rates and the flashy nature of the runoff response time increases the risk of flooding and erosion.

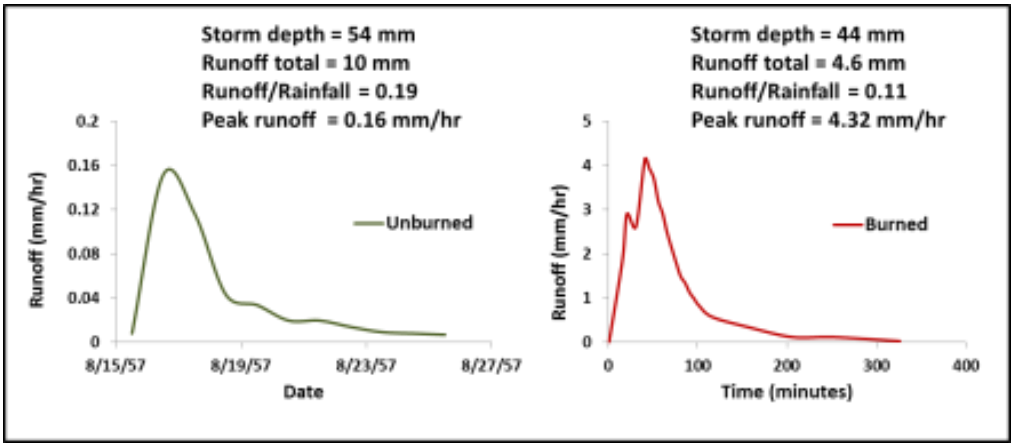

Figure 1. Pre-fire and Post-fire hydrographs recorded at Marshall Gulch. This figure illustrates the difference in storm response for unburned and burned conditions.

Hydrologic modeling is often used to anticipate the risk of flooding and erosion, and target areas for mitigating efforts. This study focuses on the KINEROS2 (Goodrich et al., 2012) hydrologic model with parameters assigned to model elements by the Automated Geospatial Watershed Assessment tool (AGWA; Canfield et al., 2005, Goodrich et al., 2005, Miller et al., 2007, Sidman et al., 2015) for landscapes disturbed by wildfire.

AGWA (see: www.tucson.ars.ag.gov/agwa or http://www.epa.gov/esd/land-sci/agwa/) is a Geographic Information System (GIS) interface jointly developed by the USDA-Agricultural Research Service, the U.S. Environmental Protection Agency, the University of Arizona, and the University of Wyoming to automate the parameterization and execution of a suite of hydrologic and erosion models (SWAT (Gassman et al., 2007) and KINEROS2 (Goodrich et al., 2012) – the latter with the Rangeland Hydrology and Erosion Model (RHEM) (Nearing et al., 2011) and/or the Water Erosion Prediction Project (WEPP) (Lane et al., 1989; Bulygina et al., 2007) for hillslope erosion options). Through an intuitive interface the user selects an outlet from which AGWA delineates and discretizes the watershed using a Digital Elevation Model (DEM). The watershed model elements are then intersected with nationally available data sets for soils and land cover to derive the requisite model input parameters. The soils geo-database provides a texture-based estimate (Rawls et al., 1982) of saturated hydraulic conductivity (Ks), and the land cover layer provides information associated with land cover types, such as percent cover, interception, and hydraulic roughness (Manning's *n*). With the addition of a burn severity map, AGWA can be used to change the existing land cover to reflect burned conditions.

To account for burn effects, AGWA reduces the percent canopy cover (CC) parameter in a land cover look up table. Currently for severe, moderate, and low burn severity the CC for a given land cover vegetation class is reduced by 50%, 32%, and 15%, respectively (Burns et al., 2013). Since AGWA increases the soil texture based Ks using equation (1) (Stone et al., 1992) as percent canopy cover (CC) increases for all land cover types, reductions in CC due to fire will therefore decrease Ks from pre-fire condition which will result in an increase in post-fire runoff.

$$Ks = Ks_{soil} * e^{0.0105*CC} \quad (1)$$

In equation (1) Ks is the saturated hydraulic conductivity (mm/hr), Ks_{soil} is the saturated hydraulic conductivity obtained from soil texture (mm/hr), and CC is the canopy cover in percent.

The key challenge for hydrologic modeling in a post-fire context is developing rules to account for fire effects. For the physically-based KINEROS2 model; the primary parameters affected by wildfire (i.e. canopy cover, interception, saturated hydraulic conductivity and hydraulic roughness) are changed as a function of the original cover type and the degree of disturbance based on a burn severity map. Although rules are in place for these parameter alterations within the AGWA framework, they are based on a limited number of hydrologic observations (Canfield et al., 2005).

The objective of this study is to use additional post-fire rainfall-runoff observations to determine if better parameter adjustments can be made for modeling post-fire runoff events. The tasks include:

- Use remotely sensed estimates of canopy cover at Marshall Gulch to better describe post-fire canopy cover conditions and the recovery period.
- Calibrate KINEROS2 using additional data collected at burned watersheds, focusing on Marshall Gulch.
- Test calibrated parameter values developed at Marshall Gulch at other burned locations in New Mexico and Colorado.
- Compare current AGWA process/results used by Burned Area Emergency Response (BAER) teams to observed data and results attained by proposed changes to the AGWA parameter estimation scheme.

2. LITERATURE REVIEW

2.1 Post-wildfire Runoff and Erosion

Wildfires change the hydrologic behavior of a forested watershed dramatically. Peak discharges and runoff volume are expected to increase given that interception is reduced when the canopy is burned, and infiltration and soil water storage are reduced when the organic layers on the forest floor are consumed (Anderson et al., 1976). With vegetation and litter cover reductions from greater than 75% pre-fire to less than 10% post-fire, surface runoff can increase over 70% and erosion can increase by three orders of magnitude (Robichaud et al., 2000). Varying increases to water quantity are possible according to Robichaud et al. (2000), however Canfield et al. (2005) found that water quantity did not increase significantly and it was the timing and magnitude of peak flow which changed more due to wildfire. An additional increase to runoff can occur if

hydrophobic soils have been created as a result of the wildfire. A hydrophobic layer can substantially increase the amount of sediment and ash which can be washed down the hillslope during a rain storm (Robichaud et al., 2000; DeBano et al., 2003).

The dramatic increase to sediment discharge can result in substantial impacts on water quality as well. Following a fire, aquatic habitats of fish, insects and amphibians are at risk as are drinking water reservoirs, and water treatment works (Meixner and Wohlgemuth, 2004).

The severity of the wildfire and the nature of the rain that falls on the burned area are the factors that most regulate post-fire runoff and erosion. Primary wildfire effects that influence watershed hydrology are: the degree to which fire consumes organic litter and wood debris, the depth of soil heating, and the extent of tree mortality (Robicaud et al., 2000). The intensity and duration of post-fire rain events determine the extent of erosion. High intensity rainfall, even at short duration can cause a high degree of erosion and runoff (Robichaud et al., 2000; Robichaud et al., 2013). In contrast, severely burned areas that experience low intensity rainfall may show little to no erosion.

Hydrologic recovery from a wildfire is dependent on vegetation re-growth. Once groundcover is reestablished to a certain extent, even with successional grasses, the amount of runoff and erosion will likely be minimal (Cerdá and Doerr, 2005). How quickly vegetation recovers is a function of several factors including rainfall, fire severity and ecosystem characteristics, making it difficult to quantify (Lentile et al., 2007). For example, Debano et al. (1996) showed that erosion rates in a ponderosa forest returned to

normal levels after 14 years for severely burned areas, after seven years for moderately burned areas, and after three years for low burn severity areas.

2.2 Hydrologic Modeling of Burned Landscapes

Due to likelihood of peak flow values increasing following a wildfire, there is concern of flooding resulting from rainstorms. Potential flooding risk is usually assessed with hydrologic modeling efforts if there is concern for life, or damage to property or infrastructure. Predictions of hydrologic changes are made at points of interest otherwise known as Values At Risk (VAR) as part of the BAER effort (Kinoshita et al., 2014).

BAER teams use a variety of hydrologic models as noted by a U.S. Forest Service survey of BAER models found in Napper 2010 (Table 1).

Table 1. U. S. Forest Service BAER model use survey noted in Napper 2010.

USGS Linear Regression Model	26%
USDA Windows Technical Release 55 (TR-55)	10%
Curve Number (CN) (various)	23%
Wildcat4 or Wildcat5	9%
Water Erosion Prediction Project (WEPP)	20%
Fire Enhanced Runoff and Gully Initiation (FERGI)	2%
Rowe Countryman and Storey (RCS)	8%
U.S. Army Corps of Engineers Hydrologic Modeling System (HEC-HMS)	2%

Several of these models have been further evaluated at eight locations by Kinoshita et al. (2014) for their ability to simulate peak flow. The models (methods) evaluated included the Rowe Countryman and Storey (RCS), USGS Linear Regression Equations, USDA TR-55, Wildcat5, and HEC-HMS. For most locations used in Kinoshita et al. (2014) model evaluations were made using flood frequency analysis for

stream flow "observations" with NOAA design storms driving the model. Calibrations using recorded rainfall and stream flow observations were presented for one location consisting of three sub-watersheds utilizing four storms (two for calibration and two for validation). This was done to illustrate the benefit of running the distributed HEC-HMS model calibration.

Pre-fire calibrations were made at four locations based on discharge. This was shown to improve post-fire simulations. No calibrations were made to post-fire conditions. It was found that peak discharge was highly variable depending on the model and the parameters selected. The RCS performed well because it is based on observed data, but because of this it is limited regionally for application. The modifiers to account for fire effects are subjective and require an *a priori* estimate of percent change in peak runoff for the USGS regression method. The TR-55 model was found to overestimate peak flows when uncalibrated. The HEC-HMS system was shown to improve when run as a calibrated distributed model as opposed to uncalibrated spatially lumped parameters. HEC-HMS used in this manner was determined to be the best choice of models by this study, if sufficient time and information was available to calibrate to pre-fire conditions. Otherwise if time and information were lacking, as is the case for typical BAER situations, the Wildcat5 model was the authors' preference for modeling peak flow. When applying this model, the pre-fire Curve Number (CN) is systematically increased as a function of burn severity (low severity CN = pre-fire CN+5, moderate severity CN= pre-fire CN+10, high severity CN= pre-fire CN+15). The efficacy of this approach was not tested against post-fire observed data.

Chen et al. (2013) evaluated the Rule of Thumb, Modified Rational Method (MODRAT), HEC-HMS Curve Number, and KINEROS2. These models were purposefully chosen for their range in complexity and diversity in approach. In their investigation all models were applied to paired burned and unburned watersheds, as well as unburned and burned conditions in a watershed that had both pre-fire and post-fire observed rainfall and runoff events. These watersheds were located in the San Dimas National Forest. The unburned watershed is 5.54 km^2 and the burned watershed is 6.16 km^2. The burned watershed was 31.6% burned in the 1953 Barrett fire, including 18.2% severely burned and 13.4% partially burned areas. The burn occurred in the upper portion of the watershed. The vegetation in these watersheds was composed of chaparral, semi-barren areas, and woodland consisting of oak, maple, and bigcone Douglas-fir. Analog data was recorded at several rain gages within the watersheds, including intensity recording gages. Stream flow measurements were taken at the outlet of each watershed.

The HEC-HMS CN approach and the KINEROS2 model both create complete hydrographs and were investigated more thoroughly by the authors. It was found that the pre-fire storms were better simulated by the HEC-HMS model and that the post-fire storms were better fit by the KINEROS2 model. Chen et al. (2013) postulate that this had to do with how surface runoff is generated in each model. KINEROS2 treats surface runoff generation as infiltration excess where the Curve Number method employed in HEC-HMS is more consistent with saturation excess run off generation. This study concluded that none of the models could accurately represent the storm flow observed and that the empirical models estimated peak flows no worse than the more physically

based models, but, the physically based models can capture important hydrologic changes that happen following a wild-fire where empirical models are less informative.

The KINEROS2 model and the SWAT model have also been used to investigate fire effects at separate basins: Starmer Gulch on the Los Alamos National Lab (LANL) was modeled with KINEROS2 and Marshall Gulch was modeled with SWAT (Canfield et al., 2005). In both cases the AGWA tool was used to transform geospatial information into input parameters. This study found that the hillslope hydraulic roughness in KINEROS2 was the parameter that was most associated to changes in peak discharge due to fire. For the SWAT model, Curve Numbers were found to change after a fire, but not dramatically, and were dependent on percent cover. The work done by Canfield et al. (2005) established the relationships between fire severity and hillslope infiltration, surface hydraulic roughness, and interception that are incorporated into the AGWA/ KINEROS2 scheme.

Values for percent canopy cover and surface roughness for differing severity of burn are shown in Table 2. Burned values were created for shrublands, evergreen forests, mixed forests and deciduous forests (Burns et al., 2013).

Table 2. Canopy cover and Manning's n for unburned and low, moderate, and high severity burns as assigned by AGWA.

Change from Unburned Condition				
Percent Cover				
Land Cover	**Unburned**	**Low Severity**	**Moderate Severity**	**High Severity**
Deciduous Forest	50	43	34	25
Evergreen Forest	50	43	34	25
Mixed Forest	50	43	34	25
Scrub	25	21	17	12
Manning's n				
	Unburned	**Low Severity**	**Moderate Severity**	**High Severity**
Deciduous Forest	0.4	0.199	0.06	0.017
Evergreen Forest	0.8	0.199	0.058	0.017
Mixed Forest	0.6	0.199	0.058	0.017
Scrub	0.055	0.01	0.005	0.003

Additional functionality has been incorporated into the KINEROS2 model since Canfield et al. (2005). Radar precipitation can now be used to drive the model (Unkrich et al., 2010), providing better estimations of the spatial variability of rainfall.

2.3 Importance of Rainfall Representation

Rainfall (precipitation in the form of snow or hail is not considered in this analysis) is the driving force behind watershed response. How rainfall is represented spatially and temporally will have a profound effect on the simulated runoff (Faures et al., 1995, Singh, 1998). The direction that a storm tracks across the watershed can also have an impact on peak flow rates (Singh, 1998). Uncertainty in precipitation estimates

propagates through rainfall-runoff models and influences uncertainties in parameter estimates (Shroter et al., 2011); meaning that if the rainfall is not adequately represented parameter adjustments made with the intent to calibrate a rainfall-runoff model could be unnecessary, if not erroneous. This is particularly important for this study because intense rainfall occurring on burned areas is extremely important in generating the post-fire peak discharge (Moody, 2011). It is often the case that a single rain gage provides information for a relatively large area. Use of information like this tends to under predict storm response for smaller events, and over predict for larger events (Hernandez et al., 2000). This is due to the relative amount of error in the recorded rainfall (Faures et al., 1995). Even by using two rain gages as opposed to one, uncertainty in model results can be reduced (Faures et al., 1995).

Radar estimates of rainfall intensity and accumulation show promise for better spatial representation of rainfall, however large errors are likely to occur if radar bias is not accounted for (Morin et al., 2006). When radar information is bias corrected it has been found to represent rainfall as well as a dense network of rain gages (Hossain et al., 2004). Although radar does provide the potential for better representation of rainfall characteristics, it still may not capture the degree of spatial variability that could be necessary to characterize convective type thunderstorms (Morin et al., 2006). The assumption of spatial uniformity within a radar grid cell (1 km by 1 degree radial grid, ranging from 0.01 - 4 km^2) could misrepresent this type of convective storms. It has been found that with convective air-mass thunderstorms, an assumption of uniformly distributed rainfall is not necessarily valid at a spatial extent greater than 5 hectares

(Goodrich et al., 1995). This study concluded that if you are modeling at that scale it is important for the model to capture rainfall variability at a high resolution.

2.4 Apparent Infiltration Rates

Infiltration rates calculated by the difference in rainfall volume and outflow volume are apparent infiltration rates (Hawkins, 1982). An increase in steady state infiltration rates with increasing rainfall intensity has been observed by Hawkins (1982), Dunne et al. (1991), Morin and Kosovsky (1995), Janeau et al. (1999), Gomez et al. (2001), Holden and Burt (2002), Mertz et al. (2002), Paige et al. (2002) and Stone et al. (2008) when measuring infiltration in this manner. This increase to the apparent infiltration rate with increasing rainfall intensity is explained by the spatial variability of the soils and vegetation in the area of interest (Stone et al., 2008). With an increase in rainfall intensity, more area will begin to contribute to runoff, and this newly contributing area will typically have a greater infiltration rate (Stone et al., 2008). According to Dunne et al. (1991) the higher parts of the microtopography of a hillslope will have higher infiltration rates due to a greater density of macropores caused by vegetation and the higher concentration of organic matter from vegetation litter that accumulates under vegetation (Abrahams et al., 1995; Bhark and Small, 2003).

Most rainfall-runoff models use a static Ks parameter values (Stone et al., 2008). Observations of rainfall simulator experiments suggest that the spatial variability of Ks and the effect that rainfall intensity apparently has on infiltration rates should not be overlooked (Stone et al., 2008, Kinner and Moody, 2008, Dunne et al., 1991). The need for different parameter values to calibrate the runoff model used by Yu et al. (1997) for

storms of varying intensity at the same location also implied the need for varying values of the Ks parameter based on rainfall intensity.

Soil physics theory predicts decreases to infiltration rate as rainfall accumulates over time due to the decrease in suction, but analysis of rainfall simulator plot data shows an increase to steady state infiltration rates with increasing rainfall intensity. Several investigators suggest the use of a rainfall intensity varying approach to modeling infiltration, and therefore runoff, should be considered (Hawkins 1982, Stone et al., 2008, Dune et al., 1991, Yu et al. 1997).

Kinner and Moody (2008) specifically conducted rainfall simulator experiments on burned areas. They hypothesized that infiltration rates were dependent on rainfall intensity and the spatial variability of how ash thickness was distributed along flow paths. A resonating conclusion made by Kinner and Moody (2008) was that processes such as infiltration must be examined at the hillslope scale to be able to predict flooding related hazards with physical models.

2.5 Literature Review Summary

The literature reviews herein indicate the potential importance of accounting for the apparent infiltration rate as a function of rainfall intensity. This finding supports the pursuit of the incorporation of rainfall intensity varying values of the Ks parameter as part of the calibration scheme outlined in section 3.4 and further developed in section 4.1. Remotely sensed estimates of canopy cover were an important part of the pursuit of rainfall varying Ks parameter values. The need to distinguish fire effects from rainfall

intensity effects required insight gained through remote sensing outlined in section 3.5 and further developed in section 4.2.

Although several studies have been conducted to assess the accuracy or validity of modeling approaches for post-wildfire assessment (section 2.2), none of these studies tested the use of burned area parameters for geographically similar burned watersheds. This is important for the practical use of hydrologic modeling in a BAER scenario, where location specific calibrations are not likely to occur. Pursuit of regional burned area parameters is outlined in section 3.6 and further developed in section 4.3. The studies presented in section 2.2 did not assess relative change analysis, which is the most appropriate way to use uncalibrated hydrologic models, as would be the typical case for BAER. An assessment of relative change results is outlined in section 3.7 and further developed in section 4.4.

3. METHODS

3.1 AGWA/KINEROS2 Framework

An ESRI ArcGIS map document was created for each study site to provide AGWA with the necessary input layers. A DEM (USGS 2014), a National Land Cover Database (NLCD) (USGS 2013) land cover layer, a Burned Area Reflectance Classification (BARC) map (Bobbe et al., 2001), and a STATSGO (NRCS 2014) soil layer were used to create AGWA parameter estimations at each location. The Burn Severity tool in AGWA was used to alter the NLCD layer using information from a BARC map in order to incorporate fire effects on the vegetation. Using AGWA, a DEM was used to delineate the watersheds, create a flow direction and a flow accumulation

grid that were in turn used to discretize each watershed into modeling elements. In the interest of comparability, the watersheds were all discretized using the criteria of a 100 acre (40 ha), contributing source area (CSA) to the head of first order channels. Once the watersheds were delineated and discretized, parameter estimations were made using the AGWA parameterization tool. This step intersects land cover layers, and soils layers which in conjunction with Look Up Tables (LUTs) and soils databases assigns parameters to the model elements. Stream channel characteristics were also assigned at this step in the process. All of the study sites were assigned a stream bed value of 0.1 for Manning's *n*, which seemed to be appropriate for ephemeral mountain streams. This value was reached by field observations at the Marshall Gulch location and the methods of Chow (1959) and Cowen (1956) as modified by Phillips and Tadayon (2006). The Hydraulic Geometry Relationship (HGR) (estimations of channel width and depth based on contributing area) was selected to be "Eastern Arizona/New Mexico" from an AGWA LUT for all study locations.

At this point a storm was chosen to drive the model. This study used observed rainfall information to drive the KINEROS2 model. KINEROS2 uses a piece-wise planar rainfall intensity field that is computed for each time step across the watershed. A projection of the centroid of each model element is intersected with the piece-wise planar rainfall field and the intensity at the intersection is applied uniformly to the model element for the interval of time the rainfall field is constant. Test runs were made by executing KINEROS2 in the AGWA environment; however calibrating efforts were made by executing the KINEROS2 model in a MATLAB environment.

3.2 Study Sites

Locations for this study were selected based on the availability of runoff and rainfall records. Ideally a stream gage was located in a stream reach very near to the perimeter of a burned area in order to capture the effects of the fire before flood attenuation occurs in unburned stream reaches. All study areas also required that rain gages and stream gages record at a high temporal frequency (less 15 minute intervals) in order to capture the rapid response of post-fire runoff induced by short duration convective storms. Locations of basins are shown in Figure 2, and spatial burn characteristics are shown in Table 3. The period of data recorded at the watershed locations are shown in Table 4.

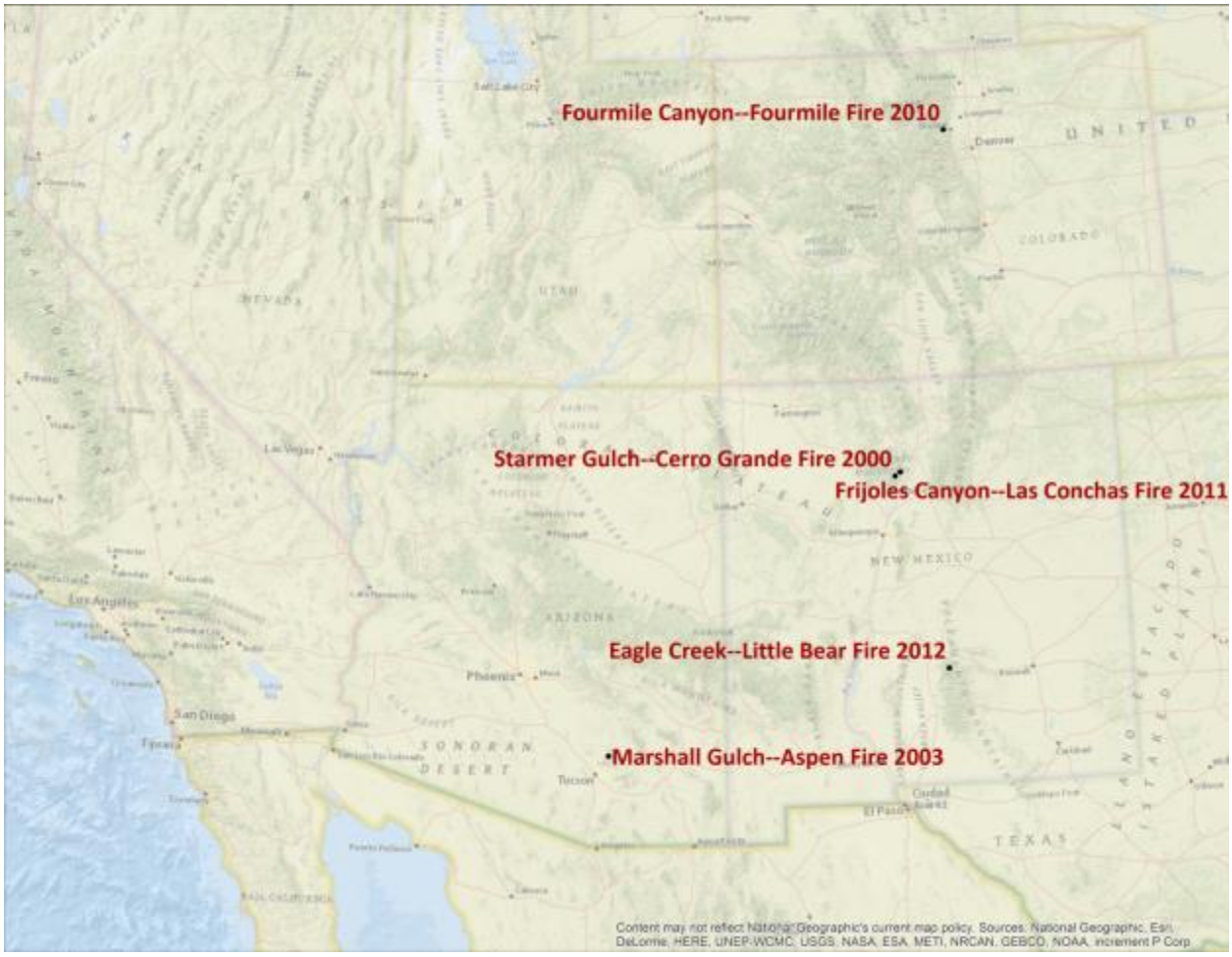

Figure 2. Locations of test basins. All test basins are located in the Southwestern United States, watershed name; fire name and year are noted on map.

Table 3. Basin and burn characteristics.

Basins and Burn Characteristics	Total Area (ha)	Unburned (ha)	Percent Burned	Low Severity (ha)	Moderate Severity (ha)	High Severity (ha)
Marshall Gulch	873	239	73	169	220	245
Starmer Gulch	314	165	48	69	19	61
Frijoles Canyon	4781	1297	73	1985	521	978
North Fork Eagle Creek	819	147	82	138	203	330
Fourmile Canyon	5416	4151	23	112	398	755

Table 4. Years of recorded stream flow and rainfall information for summer rain seasons (May-September) at test basins.

Basin	Rainfall and Stream Flow Record Dates
Marshall Gulch	2003-2014
Starmer Gulch	2000-2003
Frijoles Canyon	2012-2013
North Fork Eagle Creek	2012-2014
Fourmile Canyon	2011-2013

Marshall Gulch is 8.7 square kilometer basin located in the Santa Catalina Mountains outside of Tucson, Arizona (Figure 4). This coniferous forest watershed is defined by a stream gage operated by the Pima County Flood Control District (PCFC) downstream from the community of Summerhaven. The stream gage and rain gages operated by PCFC record information when rain is falling, or when changes in stream stage occur. The rating curve for the flow gage located at the outlet of this watershed was developed to the stage of 2.1 meters and extrapolated to 2.9 meters (Figure 3) in order to capture the maximum recorded post-fire peak flow. It was assumed that the slope of the curve remained the same as the upper end of the developed rating curve.

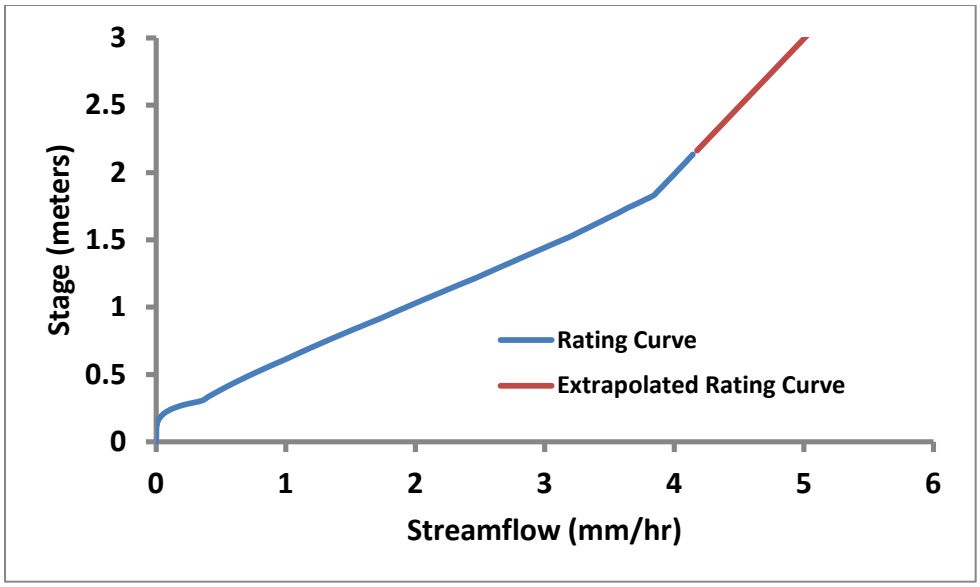

Figure 3. Rating curve relating stage to streamflow, including extrapolated values for increased post-fire peak flows.

The majority of the Marshall Gulch watershed was burned during the June 2003 Aspen Fire (Table 3). According to the STATSGO soils database (NRCS, 2014), soils on this watershed are sandy loam and very stony fine sandy loam. This test basin has the longest record of data in this study. Consequently, a large degree of attention will be given to this location. Parameters determined here will be tested at the other locations in the study to determine general applicability.

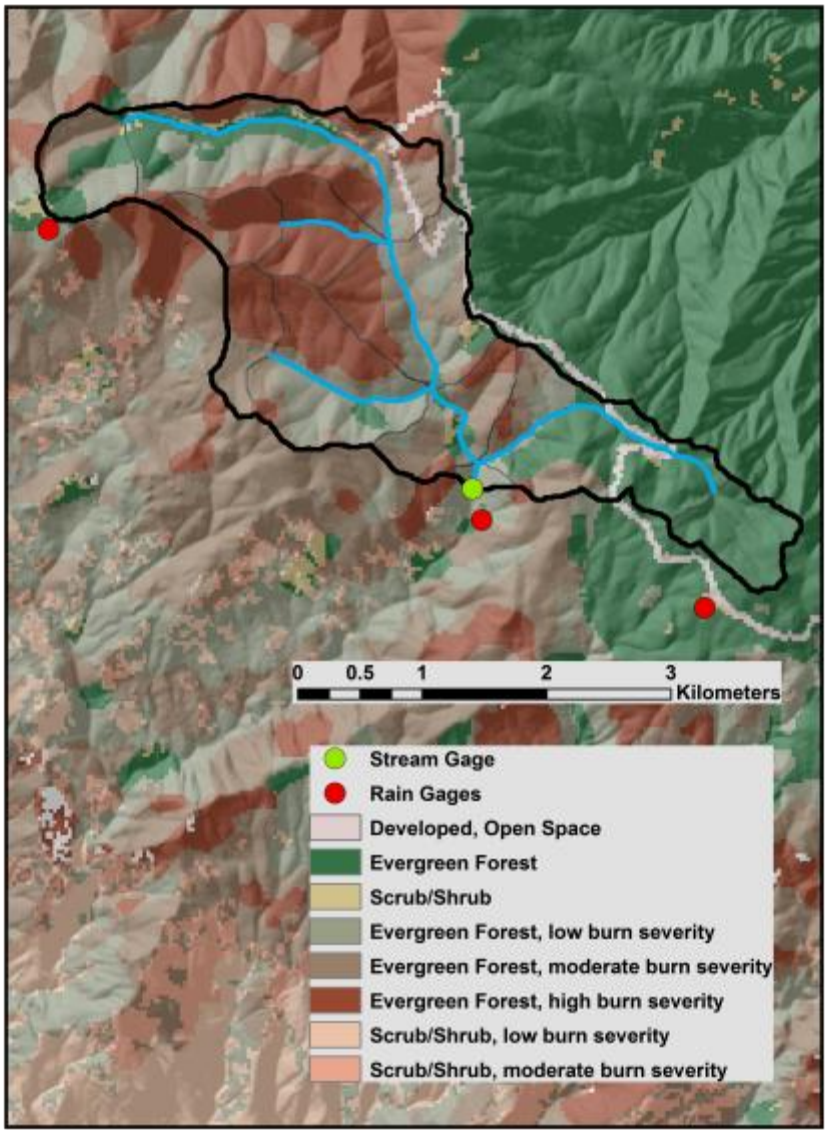

Figure 4. Marshall Gulch watershed. This map shows hillslopes, channels, land cover properties and instrument locations.

Starmer Gulch (Figure 5) located on the Los Alamos National Laboratory (LANL), New Mexico is a 3.1 square kilometer catchment that burned during the May 2000 Cerro Grande Fire. Rainfall and stream flow records were provided by LANL for the work done by Canfield et al. (2005); these same records were used for this analysis although only three of the storms used by Canfield et al. (2005) were deemed appropriate for this study. Although there were no rain gages within this basin, there are three rain gages adjacent to the watershed. This catchment is mostly a coniferous forest, with a component of shrub/scrub type vegetation, nearly half of this watershed burned (Table 3). According to the STATSGO soils database (NRCS, 2014), there are two soil groups underlying this catchment; a large area (2.3 km^2) is reported to be extremely gravely coarse sand, and the smaller area (0.8 km^2) is reported to be unweathered bedrock.

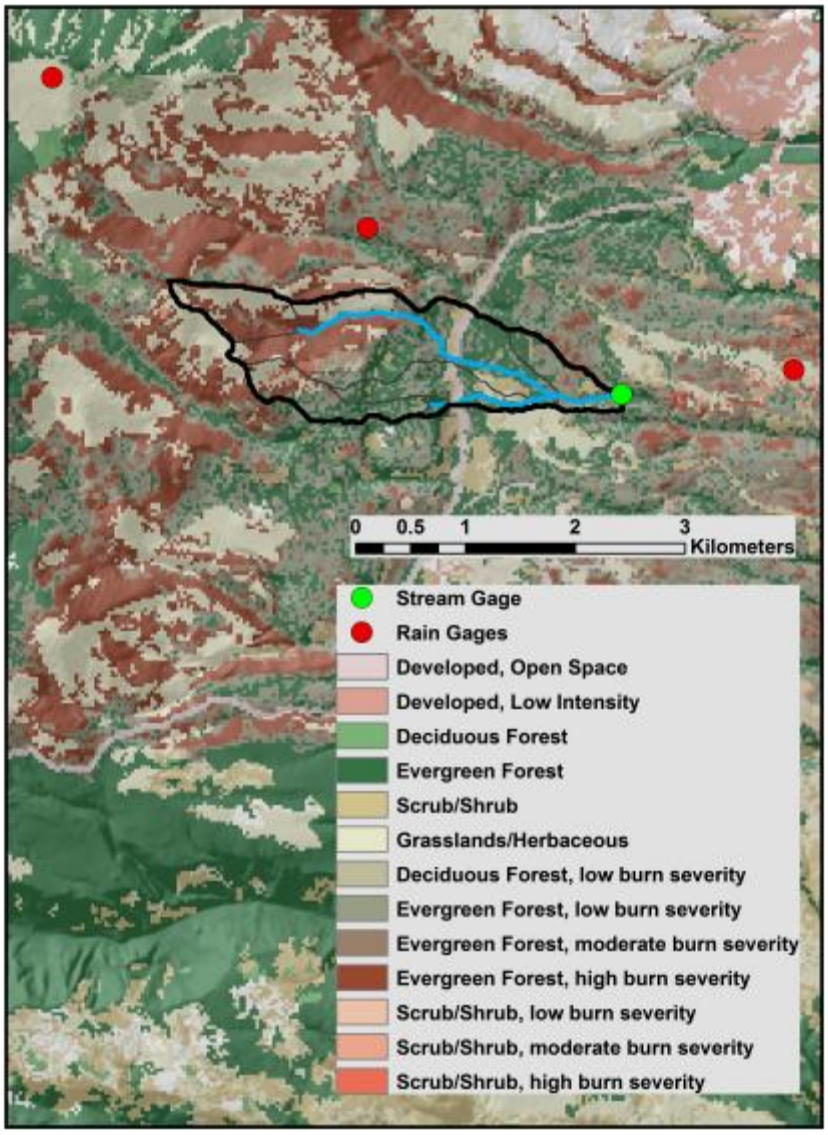

Figure 5. Starmer Gulch watershed. This map shows hillslopes, channels, land cover properties and instrument locations.

Eagle Creek (Figure 6) is a primarily coniferous basin in the Lincoln National Forest outside of Ruidoso, New Mexico. More than eighty percent of the North Fork of this basin was burned during the June 2012 Little Bear Fire (Table 3). This 8.2 square kilometer basin is defined by the USGS stream flow gage that was installed shortly following extinguishment of the fire. Rain gages were installed on the western and eastern ridges of this catchment by the USGS at the same time as the stream flow gage. STATSGO (NRCS, 2014) reports the soil to be silty clay loam on the surface, with cobbles integrated with the soil at about five centimeters depth.

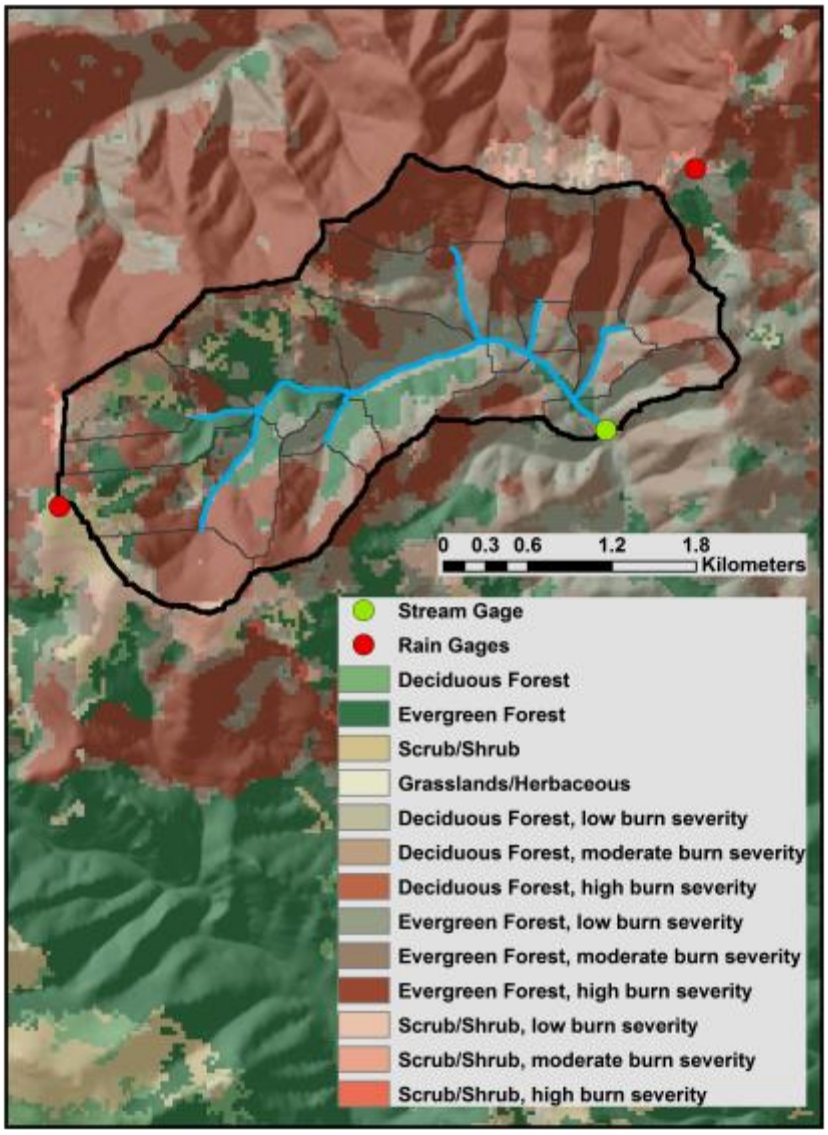

Figure 6. North Fork Eagle Creek. This map shows the locations of instruments and land cover properties.

Frijoles Canyon (Figure 7) is located in north western New Mexico, very near to Starmer Gulch. The dominant land cover type in the upper portion of this watershed was evergreen forest and the lower portion of the watershed was dominated by shrub lands with patches of forest according to NLCD (USGS, 2013). Nearly three quarters of this 48 square kilometer basin was burned in the 2011 Las Conchas Fire (Table 3). This watershed encompasses three soil units according to STATSGO, the upper and lower portions (30 km^2 and 10 km^2) of the watershed are reported to be unweathered bedrock with a smaller middle section (8 km^2) of extremely gravely course sandy loam.

The rain gages operated in this area by the USGS are likely to have not captured the spatial extent of the storms within the Frijoles Canyon watershed. For this reason, an alternate version of the KINEROS2 model was used in conjunction with AGWA. This application of KINEROS2 uses the Digital Hybrid Reflectivity (DHR) product produced by the National Climactic Data Center (NCDC) that was collected by the Albuquerque, New Mexico Next Generation Radar (NEXRAD) station. By using data collected at a USGS rain gage to bias correct radar based precipitation estimates, a more comprehensive spatial distribution of rainfall was used to drive the model (Figure 8). The rainfall intensity and therefore the rainfall accumulation was defined by a Z-R relationship (WSR-88: $Z=300R^{1.4}$) where Z=reflectivity mm^6/m^3 and R= rainfall rate mm/hr. Bias correction (in this case 3 times the radar derived rainfall rate) was performed based on accumulation at the rain gage located in the watershed, and the radar derived rainfall accumulation calculated at the corresponding radar grid bin.

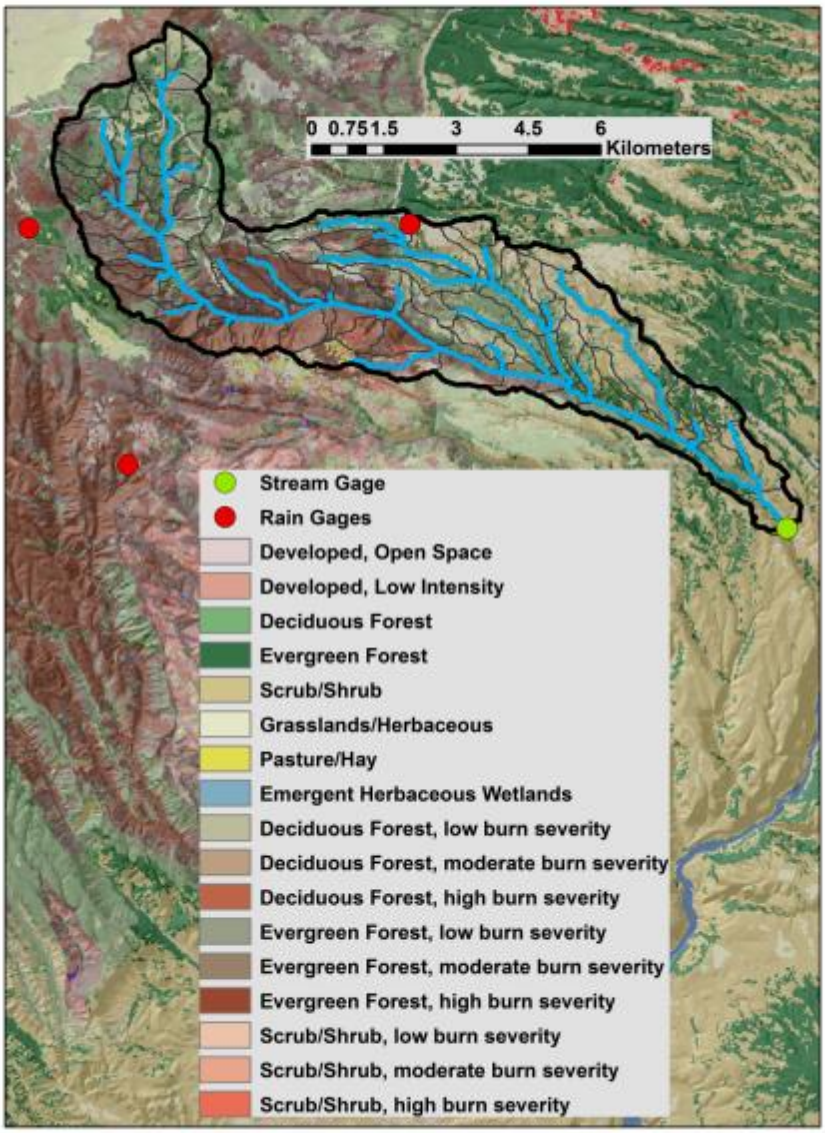

Figure 7. Frijoles Canyon. This map shows the locations of instruments and land cover properties.

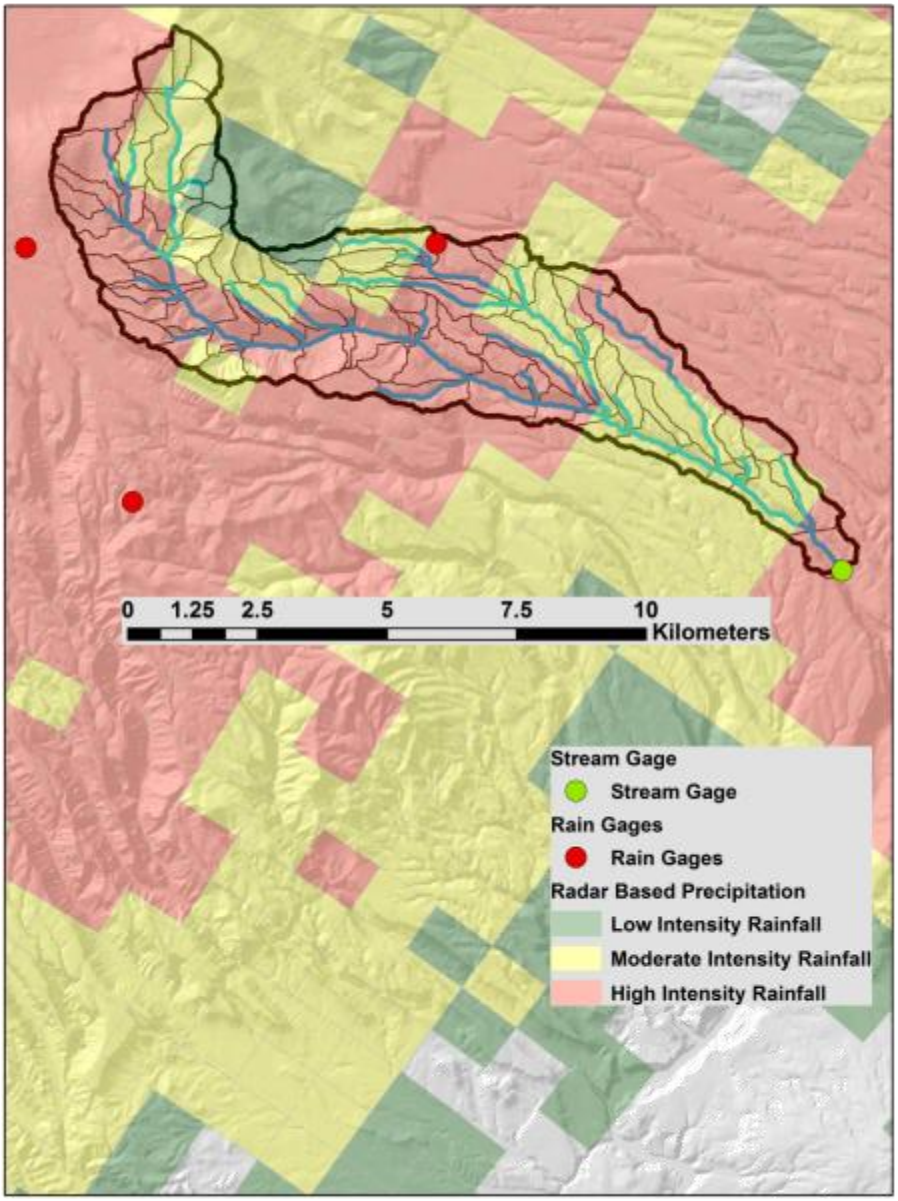

Figure 8. Frijoles Canyon radar coverage. This map shows an example radar scan to illustrate better estimation of rainfall intensity and amount relative to rain gage coverage in this larger watershed. Rainfall intensity classification for this example: Low = 0-13 mm/hr, Moderate = 13-28 mm/hr, and High = 28-50 mm/hr.

Fourmile Canyon (Figure 9) in the Front Range in Colorado is a 50 square kilometer basin, the lower portion of which (23%) was burned in the 2010 Fourmile Fire (Table 3). Although only about a quarter of this basin burned, the majority of the burn was severe and located near the outlet of the watershed, so the burn affects should be relevant. The stream flow and rain gages at this location were operated by the Urban Drainage and Flood Control District (UDFCD). According to STATSGO (NRCS, 2014), this basin includes three soil types. The lower portion includes 18 km^2 of fine sandy loam, the middle and upper sections are 26 km^2 of loam with an additional 6 km^2 of sandy loam in the upper middle region.

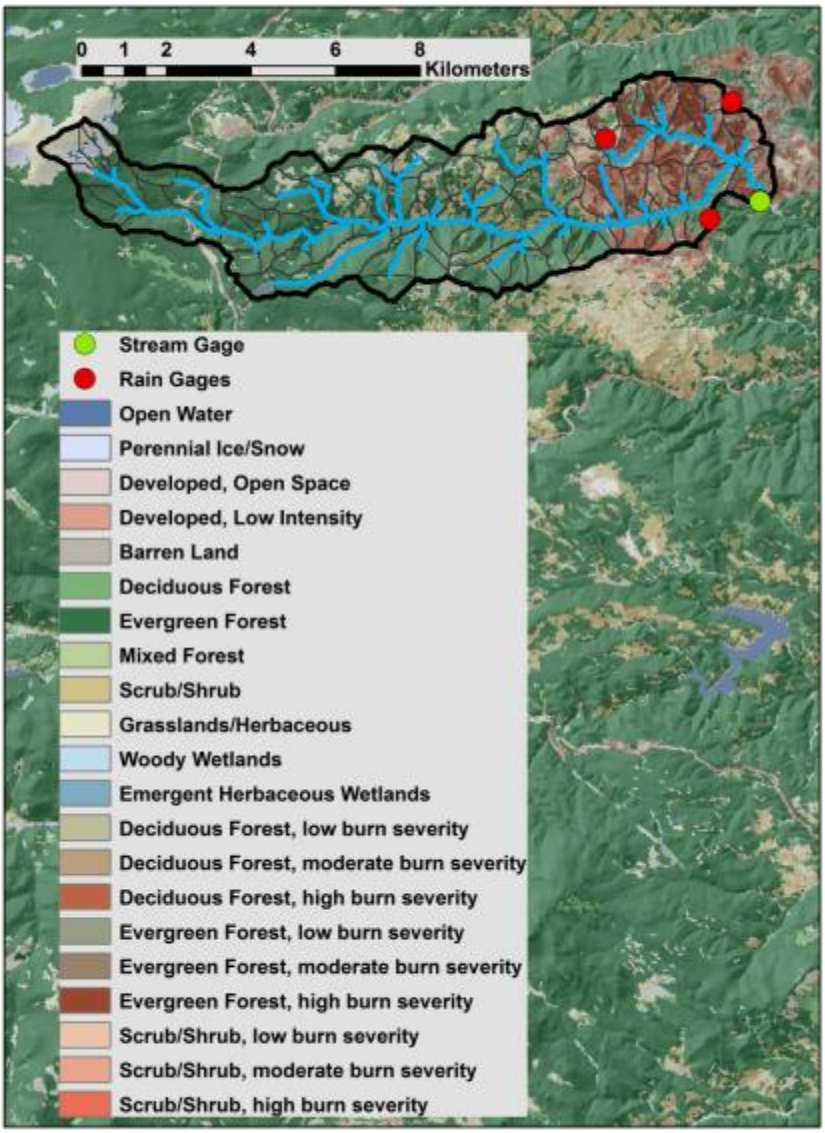

Figure 9. Fourmile Canyon. This map shows the locations of instruments and land cover properties.

3.3 Selection of storms

Several storms with varying characteristics were observed during the first couple of years following the fire at each location. This study focused on precipitation and runoff generated by summer storms, limiting the period of record to the months of June, July, August and September. As the selected watersheds have channel networks that are ephemeral or intermittent, storm flow response was easily determined and the driving rain storm was assumed to have been the most recent rainfall recorded at nearby rain gages. Initial soil moisture was accounted for and input into the model via a Saturation Index (SI). This variable can have values ranging from 0-1. The SI was estimated for each modeled storm based on the most recent rainfall accumulation. Storms that did not yield a runoff to rainfall ratio greater than five percent were culled from the Marshall Gulch post-fire storm set. This was done because events with low runoff ratios are difficult to model as the uncertainties associated with observed rainfall can be a large part of the overall runoff signal (high noise to signal ratio – Goodrich et al., 2012). In the set of storms recorded at the other watersheds and for the Marshall Gulch storm events that occurred after 2005 (two years post-burn) this criterion was not strictly adhered to in order to utilize more storms to analyze trends and develop relationships at Marshall Gulch and to test the relationships developed at Marshall Gulch on events recorded at the other basins.

The storms selected to assess wildfire effects occurred within the first two summer seasons following wildfire in order to determine the fire's effect on burned area hydrology (Table 5). At the Marshall Gulch location, several storms recorded over a

period of 11 years were analyzed to better understand rainfall intensity effects and to get a sense of how the watershed responds under unburned (recovered) conditions (Table 6).

Table 5. Post-fire storms for all basins. Basins: Marshall Gulch (MG), Starmer Gulch (ST), Frijoles Canyon (FRI), North Fork Eagle Creek (NFE), Fourmile Canyon (FM). The fire dates, storm dates, estimated initial soil moisture (SI), total rainfall accumulation, peak 30 minute intensity (I30) and runoff/rainfall ratio are listed.

Basin	**Fire Date**	**Storm Date**	**Initial Saturation (SI)**	**Total Rain (mm)**	**I30 (mm/hr)**	**Runoff/Rainfall Ratio**
MG	June 2003	7/24/2003	0.4	40.9	64.8	0.11
MG	June 2003	7/29/2003	0.5	9.7	12.4	0.27
MG	June 2003	8/7/2003	0.3	31.1	57.8	0.10
MG	June 2003	8/26/2003	0.3	11.2	13.4	0.13
MG	June 2003	7/23/2004	0.7	37.1	57.3	0.11
MG	June 2003	7/28/2004	0.6	11.5	14.2	0.22
MG	June 2003	8/13/2004	0.5	35.5	61.0	0.09
ST	May 2000	6/28/2000	0.4	11.7	23.0	0.19
ST	May 2000	7/9/2000	0.3	15.7	16.0	0.01
ST	May 2000	8/9/2001	0.4	16.8	22	0.04
FRI	July 2011	9/12/2013	0.5	39.2	16.0	0.10
NFE	June 2012	7/13/2014	0.3	38.1	37.0	0.04
NFE	June 2012	7/14/2014	0.8	15.6	19.0	0.12
FM	Sept 2010	7/13/2011	0.9	20.6	26.0	0.02

Table 6. Marshall Gulch storms. Storm dates, initial saturation (SI) total rainfall accumulation, peak 30 minute intensity (I30) and runoff/rainfall ratios.

Storm Date	Initial Saturation (SI)	Total Rain (mm)	I30 (mm/hr)	Runoff/Rainfall Ratio
7/24/2003	0.4	41.40	65.00	0.11
7/29/2003	0.5	10.12	12.85	0.25
8/7/2003	0.3	31.54	58.35	0.10
8/26/2003	0.3	11.71	13.45	0.12
7/23/2004	0.7	37.55	57.32	0.11
7/28/2004	0.6	11.95	15.13	0.21
8/13/2004	0.5	35.94	61.70	0.09
8/9/2005	0.4	25.55	29.15	0.06
7/28/2007	0.6	40.28	31.13	0.07
7/31/2007	0.6	30.99	32.87	0.26
8/8/2010	0.5	21.29	28.26	0.07
7/14/2012	0.5	24.75	27.93	0.06
7/15/2013	0.6	59.10	26.43	0.21
7/27/2013	0.6	45.21	70.78	0.02
8/12/2014	0.6	21.51	37.56	0.04
9/8/2014	0.7	50.81	31.66	0.10

3.4 Remote Sensing at Marshall Gulch

Remote sensing of the Marshall Gulch location provided insight into how realistic the AGWA look up table (LUT) estimates of percent canopy cover are for the coniferous forest land cover type, and the three levels of burn severity. Using the Normalized Difference Vegetation Index (NDVI) along with estimates of canopy cover in dense old growth forest patches at the H. J. Andrews Experimental Forest in western Oregon (assumed 100% cover) and bare ground at Marshall Gulch (assumed 0% cover) estimates of percent canopy cover were made. Polygons of coniferous forest were sampled for burned and unburned areas in and adjacent to Marshall Gulch. Pre-fire canopy cover values were determined using a satelite image from 5/15/2003, approximately one month

before the fire. Polygons of burned coniferous forest areas were sampled for the differing degrees of severity from a satelite image on 7/2/2003 immediately following the fire. Burn severity was determined by the BARC map for the Aspen fire. Spatial averages were taken within these sample polygons in order to determine the value for canopy cover to assign to the burn severity classification (eg. moderately burned coniferous foreset). An alternate LUT was created to incorporate remotely sensed canopy cover values into AGWA. Additional information pertaining to how NDVI was translated to percent cover is located in Appendix A.

Insight into canopy cover recovery also was gained through remote sensing of maximum annual NDVI for a length of time that incorporates the duration of the period of rainfall and runoff records at Marshall Gulch.

3.5 Calibration

The hillslope parameters most affected by fire are saturated hydraulic conductivity (Ks) and the hillslope hydraulic roughness (Manning's *n*). The hydraulic conductivity parameter is known to change as a result of heat from the wildfire and the nature of the vegetation that was consumed. Hillslope roughness is altered once vegetation and organic litter are consumed by wildfire (DeBano et al., 1998). Therefore these two parameters were chosen to be adjusted in calibrating the model. The AGWA/KINEROS2 modeling scheme uses multipliers to alter parameter values. This method allows for global alterations to distributed modeling elements while keeping the parameter space small. Additional parameter adjusting functionality was incorporated into KINEROS2 for this study. Parameter adjustments can now be made via multipliers

applied to specific modeling elements in addition to applying multipliers to all modeling elements in the watershed.

Two different MATLAB scripts were created for this study, each designed to apply multipliers to the Ks and Manning's *n* parameters in specified model elements in order to select optimal parameter values. These scripts used two different approaches to calibration at the rainfall event scale. One was created to calibrate by adjusting the Ks parameter to match storm runoff volume followed by adjusting the Manning's *n* parameter to match the peak flow rate. The second script was designed to best fit modeled hydrographs to observed hydrographs by running the model several times for a range of multipliers applied to the Ks and Manning's *n* parameters. Model results and observed results were used to create two dimensional error surfaces evaluated by the Nash-Sutcliffe Efficiency Coefficient (NSE) (Nash and Sutcliffe 1970) and the King-Gupta Efficiency Coefficient (KGE) (Gupta et al. 2009) objective functions. The parameter multiplier combination that generated the greatest objective function value was then selected and optimal parameter values were calculated for the event. First, calibrations were made using the runoff volume, then the peak runoff rate by adjusting the Ks parameter to reasonably match (within 10%) the runoff volume, then the Manning's *n* parameter was adjusted to match simulated to the observed peak flow rates using the same criteria. The parameters determined by this method were then used as mid points for a gridded search of the surrounding Ks and Manning's *n* parameter space using the second calibration script described above.

Special attention was given to the Marshall Gulch dataset as it had the most post-fire storms with the largest runoff/rainfall ratios (Table 5). Calibrated parameter values

determined at Marshall Gulch were tested at the other locations in this study to gain a sense of validity as well as regional applicability. In addition to calibrations made for burned land cover, calibrations were made on an artificial "uniform cover". The "uniform cover" landscape was created to model the watershed in a less distributed manner in order to highlight trends in calibrated parameters through the post-fire recovery period and to develop a relationship to describe the effect of rainfall intensity on modeled infiltration rates.

To calibrate the rainfall intensity varying infiltration rate (as observed at the outlet of the watershed) calibrating multipliers were applied to the entire watershed for the Ks parameter for the duration of the storm. The peak 30 minute rainfall intensity (I30) was chosen as the measure of rainfall intensity to correlate with the apparent infiltration rate (Ks_{ap}). Calibrations were performed for using all events from the Marshall Gulch data set (Table 6) using the "uniform cover" landscape.

Utilizing insights gained for the relationship between the I30 and the Ks_{ap}, further investigation into burned area specific parameter values was conducted. This was done by first normalizing the intensity derived infiltration rate by applying a calibrating multiplier to Ks for the entire watershed to account for the Ks_{ap}, then adjusting the Ks and Manning's *n* parameters for hillslope modeling elements that were greater than 50% burned.

3.6 Testing Regional Applicability of Apparent Infiltration Rate Calibration Technique, Burned Area Parameters and Remotely Sensed Canopy Cover

The values derived for rainfall intensity based infiltration rates (Ks_{ap}), burned area infiltration rates (Ks), burned area Manning's *n*, and remotely sensed values for canopy cover for the burned coniferous forest at Marshall Gulch were tested at all of the study sites. This was done through a series of tests using the Mean Absolute Error (MAE) of modeling results for peak flow rates compared to observed peak flow rates. This series of tests was made to show potential improvements to modeling results using remotely sensed land cover, Ks_{ap}, calibrated Ks and Manning's *n* for burned hillslopes as well as for the combined effect of these factors. A separate investigation was made to compare the Ks_{ap} to I30 relation developed at Marshall Gulch to the Ks_{ap} to I30 values derived at the other burned test basins.

3.7 BAER use of AGWA/KINEROS2: Comparison of current relative change approach to observed data and improved parameter estimates.

The typical use of the AGWA/KINEROS2 modeling scheme for BAER work is for rapid post-fire risk assessment (Goodrich et al., 2005). The rapid nature of BAER work does not allow time to calibrate hydrologic models. In most cases high-quality rainfall-runoff observations of the burned area are not available and even if they are, post-fire BAER assessments are typically conducted prior to a post-fire rainfall-runoff event. Given these constraints the relative change approach is used to illustrate the degree of change in runoff and erosion response between unburned and burned conditions as a result of a given rainstorm. The NOAA five and ten year, one hour return period design storms are used to drive the model for both the unburned and burned land cover scenarios. The degree of change in peak flow rates from unburned to burned conditions

for each of these storms provides valuable insight into the degree of risk for post-fire flooding because these are the storms most likely to occur before hydrologic recovery takes place in the watershed. These design storm depths are usually determined by NOAA atlas 14 (NOAA, 2013). The NOAA design storm rainfall depths are then translated into Soil Conservation Service (SCS) type II storms by AGWA. SCS type II storms are applicable for large interior portions of the United States outside of hurricane affected areas near the Gulf of Mexico and much of the Atlantic Coast (SCS type III storms) and the West Coast which has a strong Pacific maritime influence (SCS types I and IA storms). The number of time steps chosen to disaggregate the rainfall has implications on the peak intensity of the storm (more time steps will lead to a greater spike in peak intensity). For BAER assessments, 8-16 time steps per hour would be appropriate.

One of AGWA's unique strengths as a modeling scheme is that results can be displayed several ways: As a comparison of pre- and post-fire hydrographs, shown spatially on the map of model elements with varying degrees of change, or as a comparison table composed of information taken from the model output files. Outputs can be generated for several hydrologic components such as infiltration, peak flow rate, or total volume of flow, or for erosion characteristics like sediment discharge rates or total sediment yield.

This method of generating an anticipated change between the runoff behavior before and after a fire without calibration, then providing a way to display where differing degrees of change are expected to happen on a map, has been a very useful tool for BAER teams (T. Clifford, BAER team leader, personal communication, April, 2014).

Although the predictions in anticipated peak flow rates may not be accurate, relative change analysis provides useful insight into where to conduct initial field surveys and where to place erosion or flood mitigation efforts.

This process of using uncalibrated model runs for pre and post-fire scenarios was compared with observed flow responses recorded at Marshall Gulch for similar sized storms. Although the Marshall Gulch data set does contain one pre-fire storm event from 1957 (Figure 1) the information was recorded at a daily time step. The lack of fine scale temporal data for this pre-fire storm motivated the use of data collected ten years following the fire at Marshall Gulch as a proxy for unburned conditions. This condition is referred to as "recovered unburned". The percent changes for peak flow rates generated by the proposed changes to the AGWA parameter assignment scheme were compared to percent changes generated by the current AGWA parameter assignment scheme utilizing five year one hour SCS type II design storm disaggregated into 8, 12, and 16 time steps as well as observed storms. These results were compared to the percent change in peak flow rate calculated for the pre-fire storm of 8/16/1957 on "natural" conditions and the post-fire storm of 7/24/2003, as well as for the storm of 7/27/2013 on "recovered unburned" conditions and the same post-fire storm. Rankings of the degree of change pre- to post-fire change spatially across the modeling elements were compared to determine if the proposed changes to the AGWA scheme, or the rainstorm used altered the order in which risk was assigned to each element.

4. RESULTS

4.1 Remote Sensing at Marshall Gulch

A scan of maximum annual NDVI at Marshall Gulch gives insight into the recovery process and recovery duration that occurred following the 2003 Aspen Fire (Figure 10). Although there is inter-annual fluctuation throughout the time series of maximum annual NDVI the effects of the fire are easily seen with the decrease in the maximum annual NDVI in 2004.

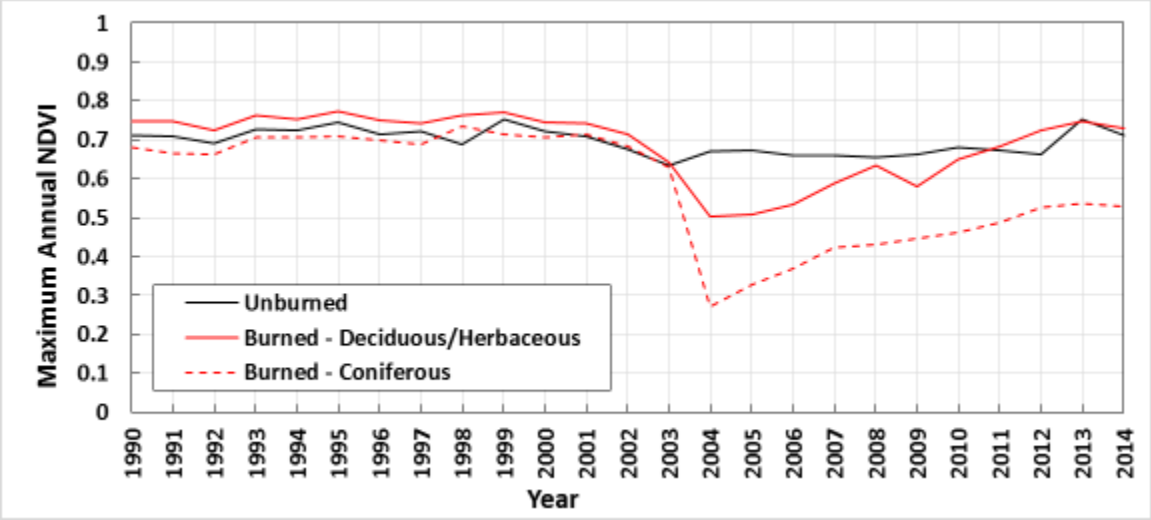

Figure 10. Maximum annual NDVI at Marshall Gulch. The black line represents unburned areas of the watershed throughout the time series, solid red line represents non-coniferous vegetation in parts of the watershed that did burn and the dashed red line represents areas in the watershed dominated by coniferous trees that burned in the Aspen Fire.

After ten years of recovery post-fire, the herbaceous category of vegetation has returned to the unburned condition where the coniferous category has yet to (Figure 10). It is possible that the coniferous trees may not return to the same degree, or dominant vegetation type that was there prior to the fire. Remote sensing does not give insight into ground cover, which is not likely to be at pre-fire levels. However, with the herbaceous canopy cover category back to normal by 2013, this landscape was considered to be hydrologically recovered or "unburned recovered" for the purpose of this study.

Differences in cover for evergreen forest derived from the NDVI based cover estimates and those provided in the AGWA LUT show notable difference in cover estimates for the severely burned category where the cover value is dropped from 25% in the AGWA LUT to 10% based on remote sensing (Table 7). Considering that the remotely sensed values for canopy cover are quite similar to the AGWA LUT values notable improvements to modeling results are not anticipated. This will be further discussed in section 5.3. Modeling results utilizing remotely sensed data are presented in sections 4.5-4.7.

Table 7. Percent cover for coniferous vegetation and associated Ks values. Percent cover estimates calculated by the NDVI method and the AGWA LUT value for unburned and burned coniferous forest conditions.

Degree Burned	AGWA LUT % Cover	Ks (mm/hr)	NDVI % Cover	Ks (mm/hr)
Unburned	50	15.3	51	15.5
Low	43	14.2	45	14.5
Moderate	34	12.9	31	12.5
Severe	25	11.8	10	10.1

4.2 Uniform Cover Calibration at Marshall Gulch

Results determined by KGE and NSE were comparable if not identical, for this reason only the NSE will be reported. The actual landscape conditions used for this part of the analysis breaks down into three time frames: 2003-2004 as "burned" years, 2005-2012 as "midyears" and 2013-2014 as "unburned recovered" (Table 8).

An example of a gridded search of the parameter space used to determine optimal parameter values is presented in Figure 11, with a corresponding plot of rainfall input, observed hydrograph and a simulated hydrograph using optimal parameters is shown in Figure 12.

Table 8. Optimal values for Ks and Manning's *n* parameters determined by volume then peak and gridded search calibration schemes for Marshall Gulch uniform cover condition. Rows highlighted in red are considered "burned", light green are "midyears' and darker green are "unburned recovered".

Storm date	I30 (mm/hr)	Runoff/ Rainfall Ratio	**Volume then peak calibrations (optimal values)**		**Gridded search calibrations (optimal values)**		
			Ks (mm/hr)	Manning's *n*	Ks (mm/hr)	Manning's *n*	NSE
7/24/03	65.00	0.11	27.18	0.50	20.65	0.90	0.85
7/29/03	12.85	0.25	0.72	0.15	0.91	0.15	0.87
8/7/03	58.35	0.10	22.62	0.60	18.12	0.80	0.89
8/26/03	13.45	0.12	1.00	0.25	1.81	0.10	0.94
7/23/04	57.32	0.11	31.71	0.45	27.18	0.55	0.83
7/28/04	15.13	0.21	1.09	0.20	1.81	0.15	0.80
8/13/04	61.70	0.09	24.46	0.35	24.46	0.35	0.72
8/9/05	29.15	0.06	9.06	0.50	9.09	0.50	0.39
7/28/07	31.13	0.07	13.59	1.00	16.31	0.70	0.49
7/31/07	32.87	0.26	10.87	0.50	10.87	0.50	0.39
8/8/10	28.26	0.07	4.98	0.50	4.98	0.60	0.70
7/14/12	27.93	0.06	19.93	0.35	11.78	0.80	0.92
7/15/13	26.43	0.21	4.53	0.90	5.44	0.90	0.59
7/27/13	70.78	0.02	38.05	0.80	38.05	0.80	0.79
8/12/14	37.56	0.04	9.97	1.00	13.59	0.80	0.79
9/8/14	31.66	0.10	9.06	1.50	16.31	0.70	0.13

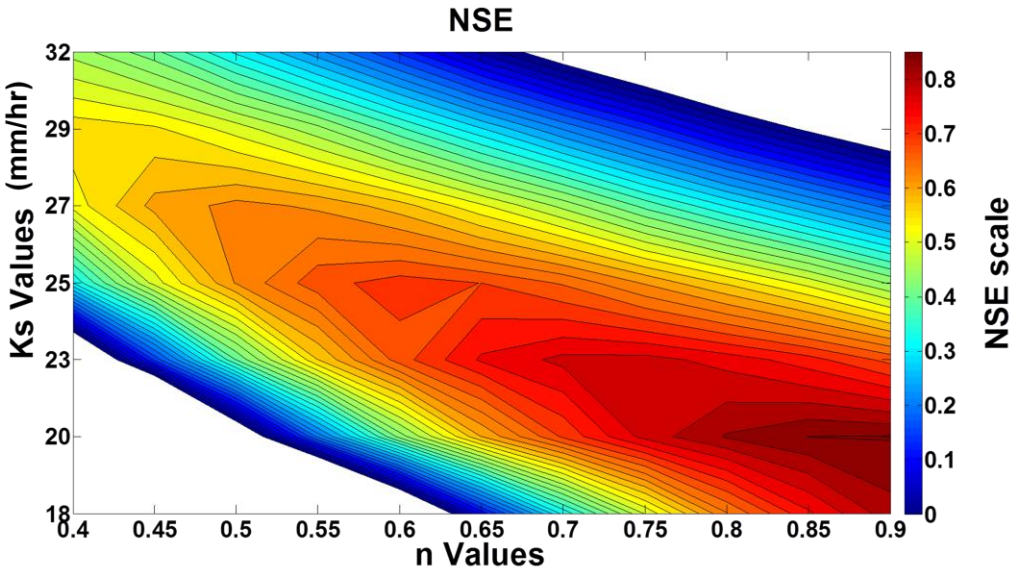

Figure 11. Error surface for the storm of 7/24/2003 at Marshal Gulch generated using the Nash-Sutcliffe Efficiency coefficient. This figure shows a gridded search of the Ks (Ks values, mm/hr) and Manning's *n* (n values) parameter space.

The Manning's *n* values used for the simulations that created the error surface shown in Figure 11 were purposefully limited to a maximum value of 0.9. This was done because values greater than this would be very unrealistic, especially in a post-fire environment. Calibrated roughness values this great indicate that shallow sub-surface storm flow may be occurring and large Manning's *n* values are accommodating for the increased friction in the model. The diagonal trend in optimal values indicates parameter interdependence.

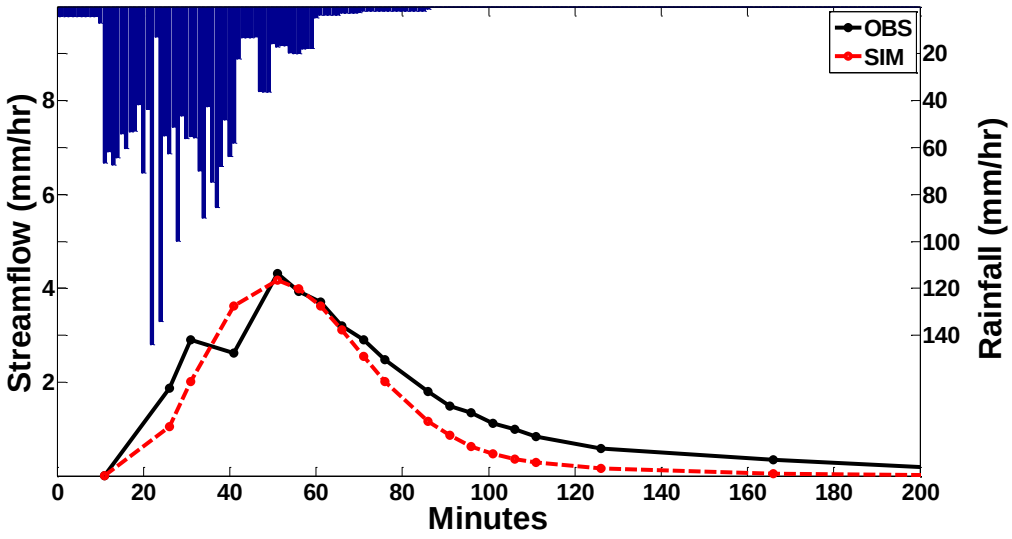

Figure 12. Observed hyetograph and hydrograph with simulated hydrograph for the Marshal Gulch storm of 7/24/2003 using optimal parameters selected (Figure 10). The simulated hydrograph fit the observed hydrograph with a Nash-Sutcliffe Efficiency coefficient of 0.85.

Figures 13-14 show the best fit and the worst modeled hydrographs for the events listed in Table 8. The KINEROS2 model is able to capture the post-fire storm of 8/26/2004 well. Figure 13 shows the storm of 9/8/2014 that includes worst fit simulated hydrograph, where simulated flow ends several hours earlier than the observed flow. As the forest at this point in time can be considered hydrologically recovered, the longer hydrograph recession is expected as with possible reestablishment of lateral subsurface flow or very slow flow through re-accumulated litter. It is also expected that the KINEROS2 model will not capture a longer hydrograph recession as it only represents runoff and therefore stream flow generation as infiltration excess.

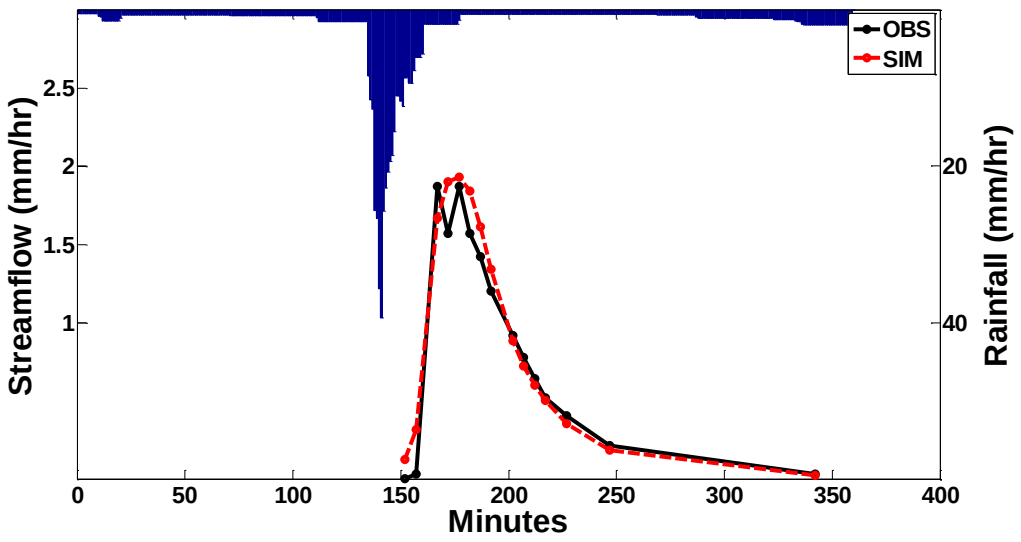

Figure 13. Observed hyetograph and hydrograph with simulated hydrograph for the storm of 8/26/2004. This was the best fit simulation with a Nash-Sutcliffe Efficiency coefficient of 0.94.

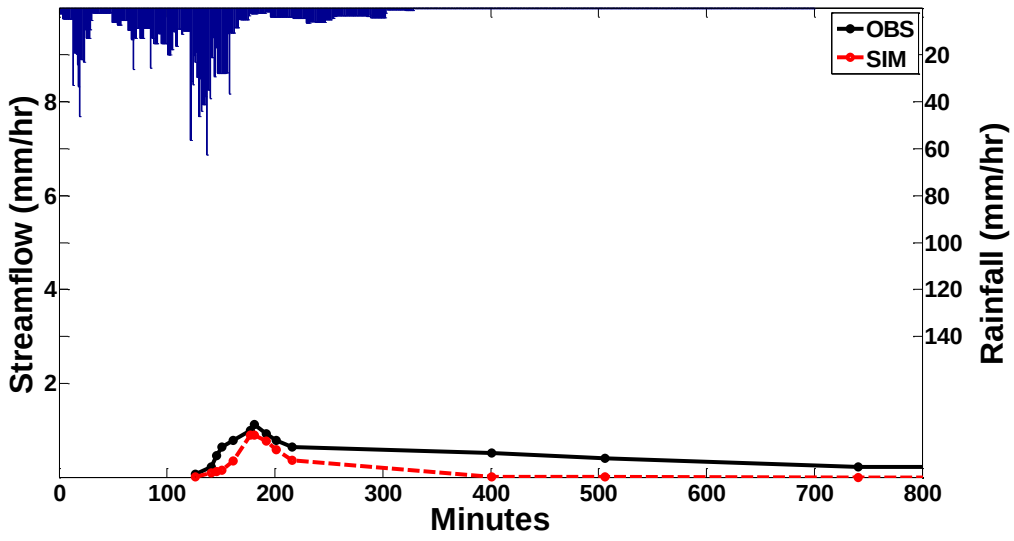

Figure 14. Observed hyetograph and hydrograph with simulated hydrograph for the storm of 9/8/2014. This was the worst fit simulation with a Nash-Sutcliffe Efficiency coefficient of 0.13.

Figures 15-19 utilize the "uniform cover" calibration information presented in Table 8 to develop the relationship between rainfall intensity (I30) and the apparent infiltration rate (Ks_{ap}), and to illustrate trends in the calibrated Ks and Manning's *n* parameters. In Figures 15 and 17 the correlation between rainfall intensity and calibrated infiltration rates and hillslope hydraulic roughness are shown. Figure 16 relates the calibrating Ks multiplier to the I30 (mm/hr) for the development of the Ks_{ap}: I30 relationship.

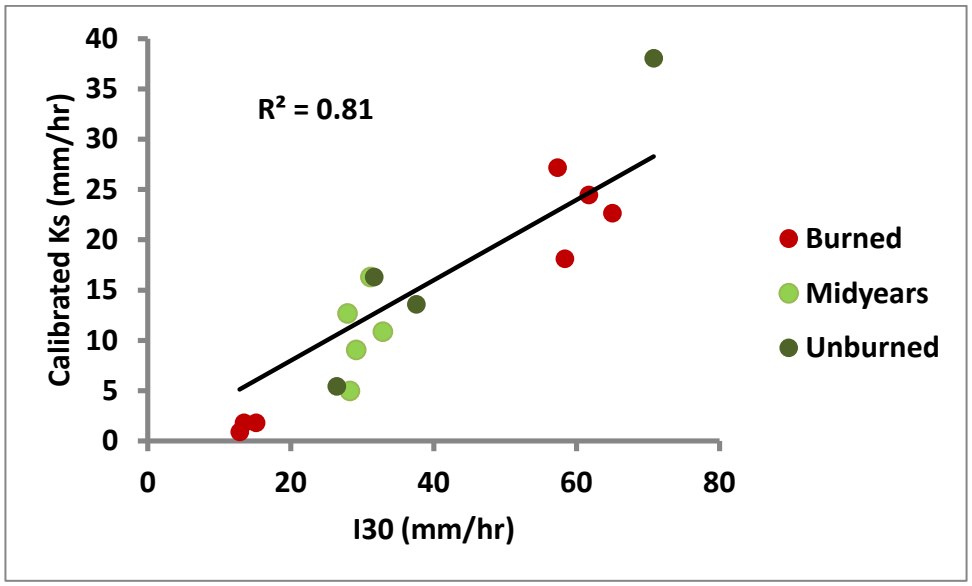

Figure 15. Correlation between rainfall intensity (I30) and infiltration rates (Ks). A significant ($p<0.05$) correlation ($r=0.92$) was established between calibrated Ks values and peak 30 minute rainfall intensity (I30).

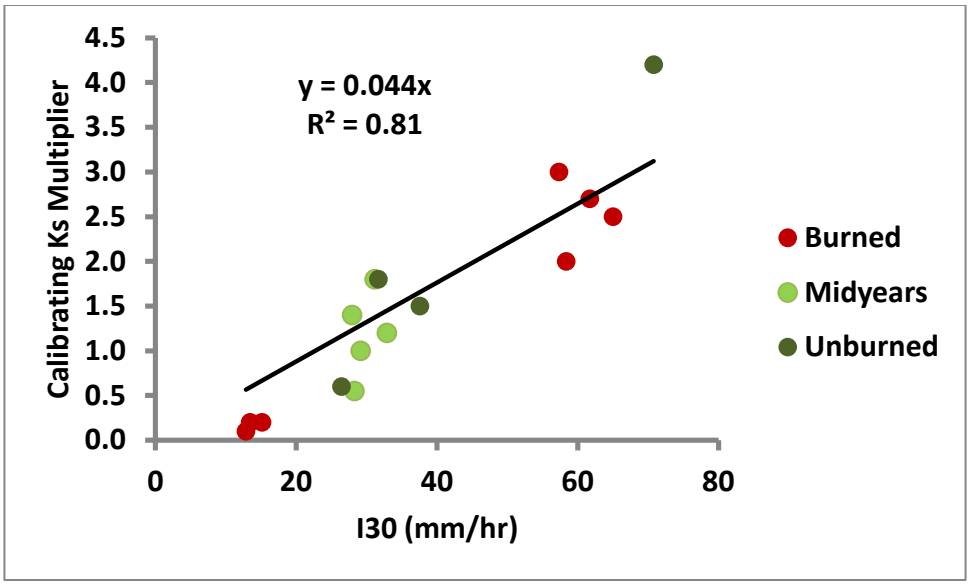

Figure 16. Linear relation for the multipliers used to calibrate the Ks parameter and the peak 30 minute rainfall intensity (I30).

The calibrated value for Ks is more a function of rainfall intensity than the condition of the landscape in terms of the fire according to Figure 15. With the calibrated Ks values ranging from 1 mm/hr to 27 mm/hr during the first two years following the fire, no relationship for calibrated Ks values and burned area characteristics could be determined. However, the strong significant correlation between the I30 and the calibrated Ks values does indicate that rainfall intensity should be considered when establishing Ks parameter values when running the KINEROS2 model for a given rainfall event. The linear relationship for the I30 (mm/hr) to Ks is assumed to represent the apparent infiltration rate, referred to as Ks_{ap} (mm/hr). The multiplier relationship used to adjust for the Ks_{ap} is shown in Figure 16 with the linear relation expressed by Equation 2.

$$Ks_{ap}multiplier = 0.044 * I30 \qquad (2)$$

The regressions used to describe changes to the apparent infiltration rate related to rainfall intensity were forced to go through the origin, as it does not make sense to have a negative infiltration rate.

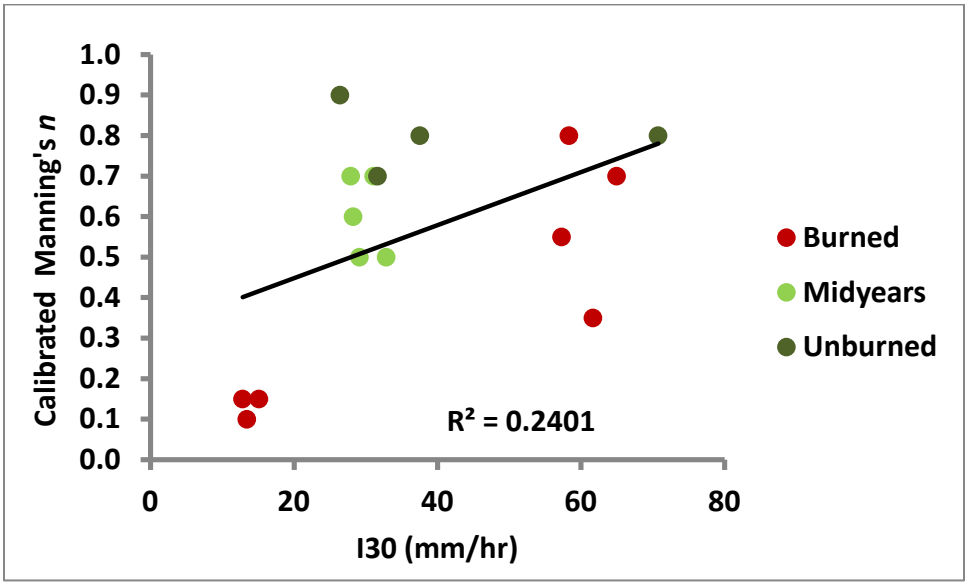

Figure 17. Correlation between rainfall intensity (I30) and Manning's *n* (r=0.49). Calibrated surface roughness values are not strongly associated with rainfall intensity. This correlation is not significant.

In Figures 18 and 19 trends in calibrated parameter values over the duration of the Marshall Gulch data set are shown.

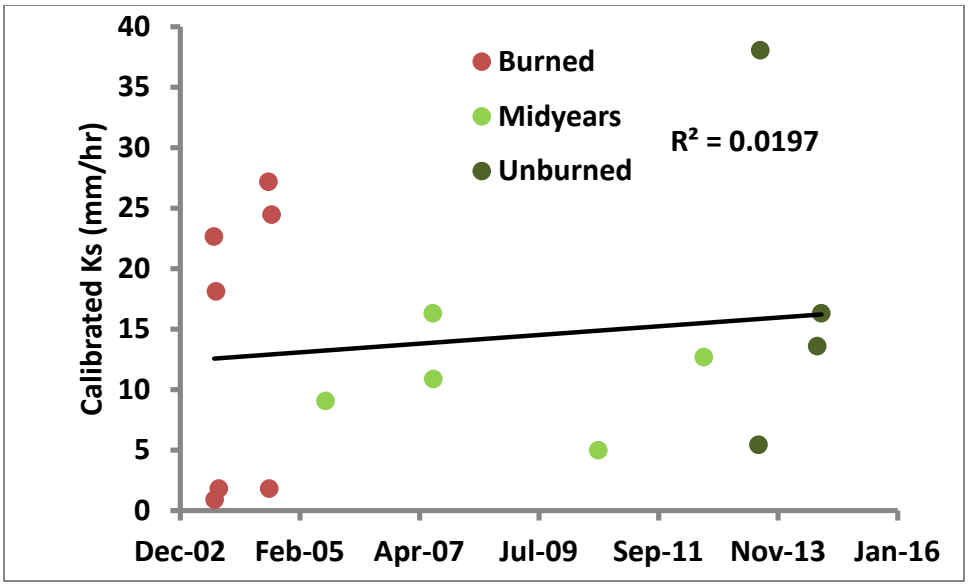

Figure 18. Correlation between calibrated Ks values and time since fire. A weak correlation (r=0.14) was determined for calibrated Ks values as a function of time, showing that the calibrated Ks values are not strongly associated to vegetative recovery. This correlation is not significant.

The correlation between the calibrated Ks values and time is very weak and not significant. The trend shown in Figure 18 is somewhat misleading as the calibrated Ks values are much more associated with rainfall intensity than the recovery time of the vegetation in the watershed.

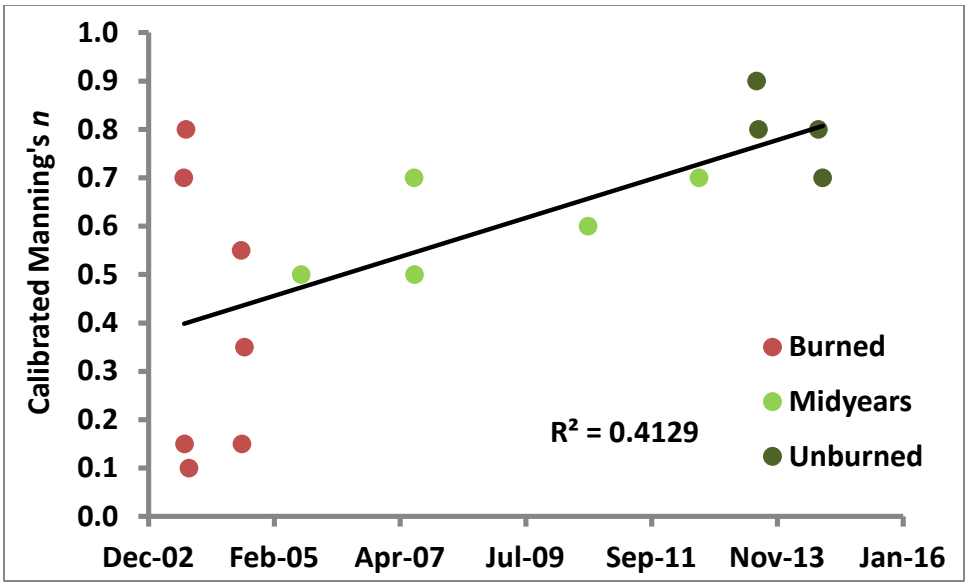

Figure 19. Significant Correlation ($p<0.05$) between Manning's *n* and time since fire ($r=0.64$). Calibrated roughness values were quite variable immediately following the fire.

Figure 19 shows that there is a significant correlation between the calibrated values for Manning's *n* and the time since the fire. This makes sense in terms of vegetative recovery. The wide range of calibrated values for Manning's *n* immediately following the fire seems to be a reasonable result as fire disturbance could cause a varying degree of roughness on the landscape. This could also be a result of parameter interdependence and the inability of this study to determine what exactly is causing the variation in Ks values, and therefore Manning's *n* values.

4.3 Uniform Cover Calibration at Other Locations

Uniform cover conditions were investigated at Starmer Gulch, Frijoles Canyon, North Fork Eagle Creek, and Fourmile Canyon to determine the regional applicability of calibrating multipliers used to account for Ks_{ap} developed at Marshall Gulch. Figure 20 shows a scatter plot of these calibrating Ks multipliers and their corresponding I30, as

well as the calibrating multipliers for the storms recorded at Marshall Gulch. With very few data points generated from storms at the various locations, it was not expected that the R^2 value be very strong for the linear regression determined by the calibrating Ks multipliers used at the other burned basins to account for the I30. However, forcing the regression through the origin yielded an R^2 that was not valid. Further investigation showed that if the regression for the other locations Ks and I30 was not forced to go through the origin it yielded a slope that appeared quite different (Figure 21). However, the results from a Johnson-Neyman test (D'Alonzo, 2004) determined that the regressions for Marshall Gulch and the other test basins were not significantly different from each other. It can be seen in Figure 21 that all but one data point, which was part of the other basins data set, lie in the prediction interval based on the unrestricted regression of the Marshall Gulch data. Furthermore, it can be seen in Figure 22 that the restricted Marshall Gulch regression lies within the confidence intervals of the unrestricted Marshall Gulch regression.

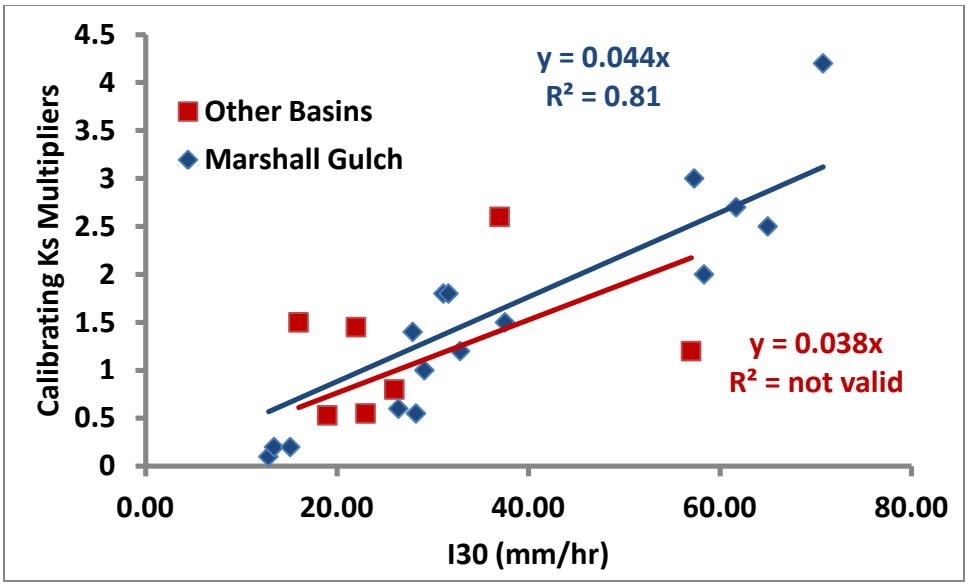

Figure 20. The relation of Marshall Gulch calibrating Ks multipliers and I30 (mm/hr) and the relation of calibrating Ks multipliers and I30 (mm/hr) used at the other test basins. This plot shows that the trend in calibrated Ks values related I30 (mm/hr) for data taken from all of the burned basins is similar to the relation developed at Marshall Gulch.

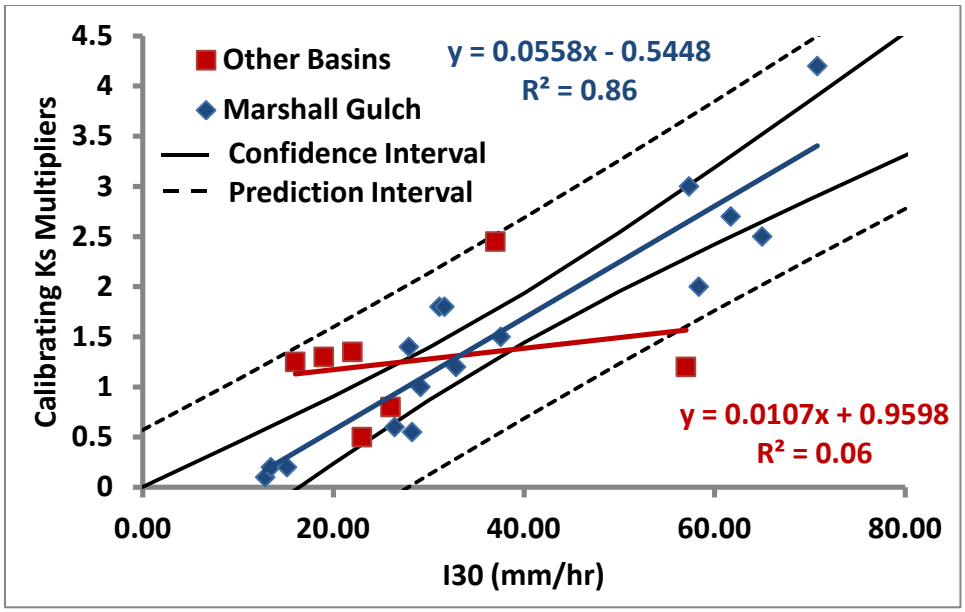

Figure 21. The relation of Marshall Gulch calibrating Ks multipliers and I30 (mm/hr) and the relation of calibrating Ks multipliers and I30 (mm/hr) used at the other test basins, where the regressions have not been forced through the origin. Prediction and confidence intervals for the Marshall Gulch regression are shown.

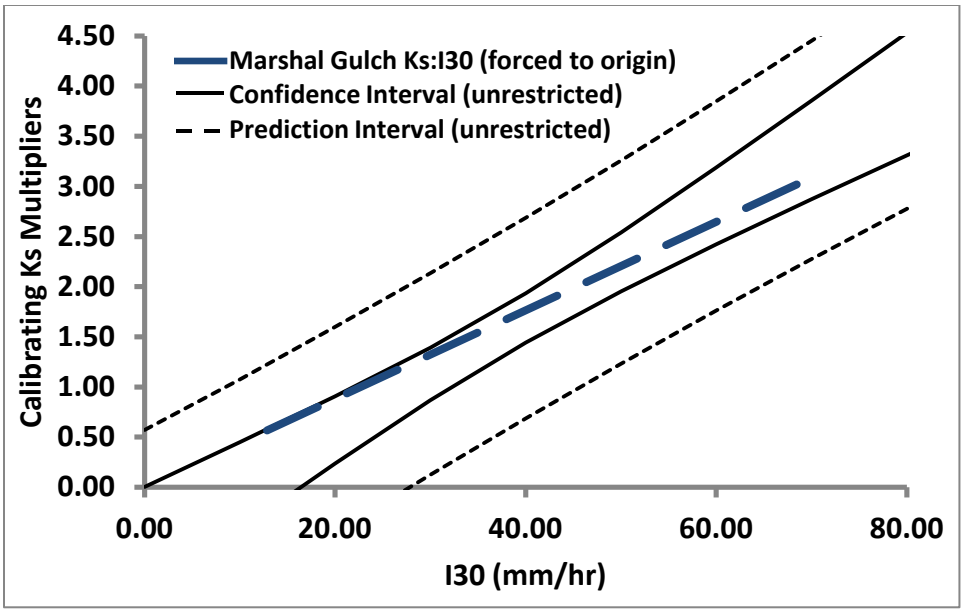

Figure 22. The relation of Marshall Gulch calibrating Ks multipliers and I30 (mm/hr) (forced to the origin) shown as it relates to the prediction and confidence intervals developed for the Marshall Gulch regression that was not forced through the origin.

4.4 Burned Area Calibration at Marshall Gulch Considering Apparent Infiltration Rates

Considering the Ks_{ap} to I30 relation shown in Equation 2 further calibrations were made to the burned areas within Marshall Gulch. This was done by applying a calibrating multiplier to the entire watershed for Ks_{ap} based on Equation 2 and the I30 calculated for the observed event, then applying multipliers to calibrate the Ks and Manning's *n* parameters in modeling elements that were greater than 50% burned. Results are shown in Table 9 for calibrations performed on the landscape defined by the default LUT in AGWA. These model runs were performed on distributed model elements, and did not produce hydrographs that reasonably matched the observed hydrographs. For this reason the ratio of simulated/observed peak flows was used as a

measure of model performance. Figure 23 shows an example of a simulation focused on matching the observed peak flow rate rather than complete hydrograph.

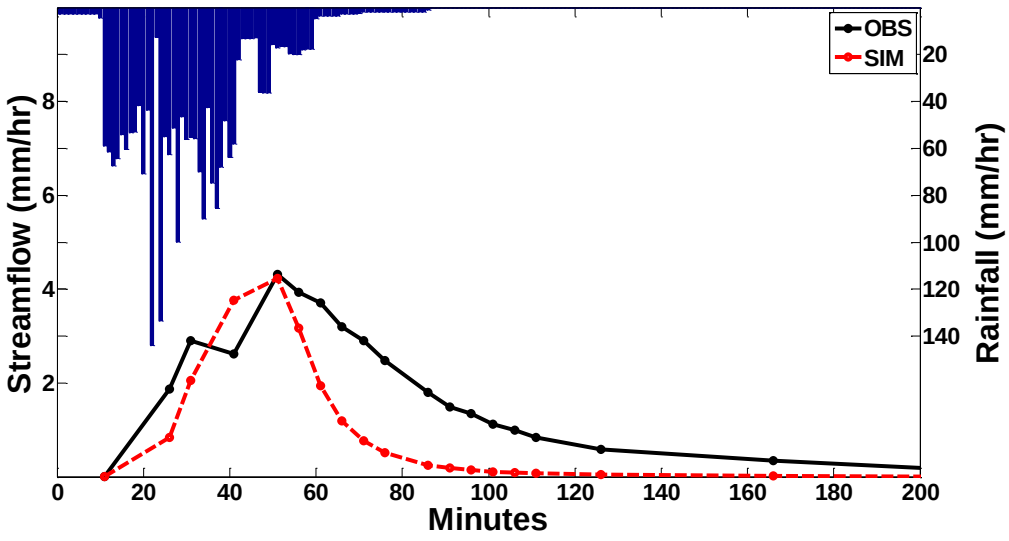

Figure 23. Observed hyetograph and hydrograph with simulated hydrograph for the storm of 7/24/2003 at Marshall Gulch using distributed modeling elements and the burned landscape. This simulation is focused on matching peak flow rate rather than maximizing the NSE.

Table 9. Multiplier values applied to the entire Marshall Gulch watershed and the burned areas within Marshall Gulch using the land cover values native to AGWA. The ratio of simulated to observed peak flow rates is provided as a measure of model performance.

Storm Date	I30 (mm/hr)	Runoff/ Rainfall ratio	Global Ks multiplier	Burned Area Ks multiplier	Burned area Manning's *n* multiplier	Simulated/ observed peak flow rates
7/24/2003	64.80	0.11	2.95	0.85	0.6	1.08
7/29/2003	12.44	0.26	0.55	0.10	0.30	1.10
8/7/2003	57.88	0.10	2.64	1.00	1.00	0.97
8/26/2003	13.45	0.13	0.61	0.30	0.50	1.09
7/23/2004	57.32	0.11	2.61	1.2	1.5	0.93
7/28/2004	14.31	0.22	0.65	0.40	0.40	0.79
8/13/2004	61.05	0.09	2.87	1.1	1.1	0.98

The multipliers used to adjust burned area parameters shown in Table 8 seem to be associated with the rainfall intensity of the storm. Smaller multipliers used for less intense storms and larger multipliers used for more intense storms for burned areas seems to indicate that the two tiered calibration scheme did not achieve the goal of isolating the effect of the fire on hillslope parameters from the rainfall intensity effect. Further refinements for how calibrating Ks multipliers are applied spatially and temporally could reveal more meaningful results, and are discussed further in section 5.4

4.5 Burned Area Calibration at Marshall Gulch Considering Apparent Infiltration Rates and Remotely Sensed Land Cover

An alternative land cover LUT was created to utilize the NDVI derived cover values for the Marshall Gulch watershed. These tests were done in the same manner described in section 4.4, using a global multiplier to account for rainfall intensity then applying multipliers to burned areas specifically. Results for these calibrations are shown in Table 10.

Table 10. Multiplier values applied to the entire Marshall Gulch watershed and the burned areas within Marshall Gulch using NDVI derived land cover values. The ratio of simulated to observed peak flow rates is provided as a measure of model performance.

Storm Date	I30 (mm/hr)	Runoff/ Rainfall ratio	Global Ks multiplier	Burned Area Ks multiplier	Burned area Manning's *n* multiplier	Simulated/ observed peak flow rates
7/24/2003	64.80	0.11	2.95	0.92	0.90	1.04
7/29/2003	12.44	0.26	0.55	0.15	0.15	1.05
8/7/2003	57.88	0.10	2.64	1.05	1.00	1.02
8/26/2003	13.45	0.13	0.61	0.30	0.50	1.18
7/23/2004	57.32	0.11	2.61	1.30	1.50	1.04
7/28/2004	14.31	0.22	0.65	0.40	0.40	0.90
8/13/2004	61.05	0.09	2.87	1.2	1.30	1.03

Similar to what was seen in Table 9, the results shown in Table 10 show that the rainfall intensity (I30) seems to be a factor in burned area parameter calibration results. Even when using remotely sensed estimates for land cover values, smaller calibrating multipliers were used for less intense storms and larger calibrating multipliers were used for more intense storms for burned areas for the Ks parameter. Given that the remotely sensed canopy cover values were quite close to the AGWA LUT values for coniferous forest and burned coniferous forest, this similarity is not surprising. The use of remotely sensed canopy cover values for improved model results should be further investigated, and is further discussed in section 5.1.

4.6 Using Marshall Gulch Calibrated Parameters and AGWA Default Parameters at All Locations

Several model runs were made to examine whether improvements to modeling results for peak flow rates for the proposed changes to the AGWA parameter estimation scheme would be realized. The relation between rainfall intensity and apparent

infiltration rates (Equation 2), remotely sensed estimates of land cover, and parameter adjustments made for burned areas developed at Marshall Gulch were tested at all burned locations. This was done in a series of comparisons of simulated peak flow rates to observed peak flow rates utilizing the Mean Absolute Error (MAE) as a measure of model performance. Table 11 and Figures 24-29 show results and the associated MAE for the different input parameter scenarios. Table 11 includes the observed mean peak flow rate to compare with the MAE for the various simulations.

Table 11. Mean Absolute Error (MAE in mm/hr) for modeled peak flow rates and observed mean peak flow rate. This table shows the error associated with model runs for AGWA default parameters, remotely sensed land cover, parameter adjustments made for the apparent infiltration rate (Ks_{ap}), and for parameter adjustments made to burned area infiltration rates (Ks) and hillslope hydraulic roughness (Manning's *n*).

MAE for simulated peak flow rates			
Parameter scenarios	**Observed mean peak flow rate (mm/hr)**	**AGWA/NLCD land cover MAE (mm/hr)**	**Remotely sensed land cover MAE (mm/hr)**
Default	3.2	6.3	6.7
Accounting for Ks_{ap}	3.2	2.1	2.4
Accounting for Ks_{ap} + burned area Ks * 0.9, Manning's *n* * 0.9	3.2	2.4	2.7
Accounting for Ks_{ap} + burned area Ks * 0.7, Manning's *n* * 0.9	3.2	3.4	3.8
Accounting for Ks_{ap} + burned area Ks * 0.8, Manning's *n* * 1	3.2	2.7	3.1

Figure 24 shows the results for simulations performed using the land cover values native to AGWA and Figure 25 shows results using the remotely sensed land cover value estimates. The MAE value of 6.7 for simulations using remotely sensed land cover values was larger than the MAE value of 6.3 obtained from simulations using the land cover values native to the AGWA scheme indicating that in this case remotely sensed cover values do not improve modeling results.

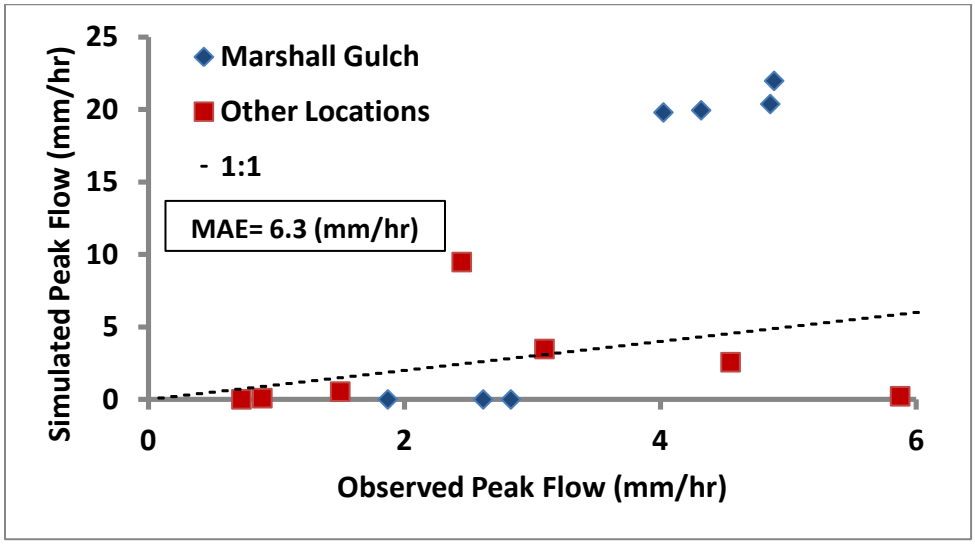

Figure 24. Comparison of simulated and observed peak flow rates using AGWA default cover estimates.

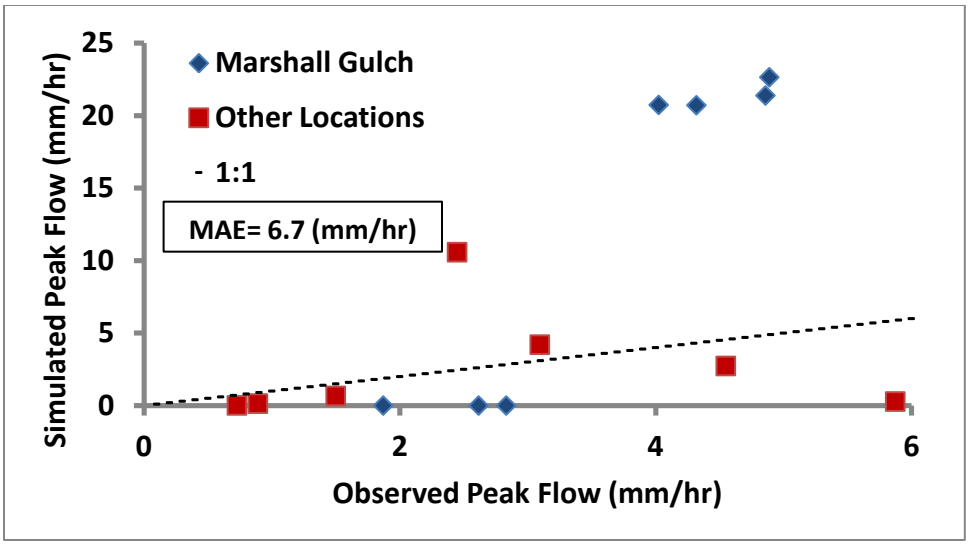

Figure 25. Comparison of simulated and observed peak flow rates using remotely sensed cover estimates.

Figures 26 and 27 show modeling results that incorporate the use of Equation 2 to account for the apparent infiltration rate that is associated to the peak 30 minute rainfall intensity. Figure 26 shows results for model runs performed using AGWA default land cover values, yielding an MAE of 2.1. This showed a vast improvement in results compared to simulations that did not account for rainfall intensity. Figure 27 shows an MAE value of 2.4 indicating that the use of remotely sensed land cover values did not further improve modeling results.

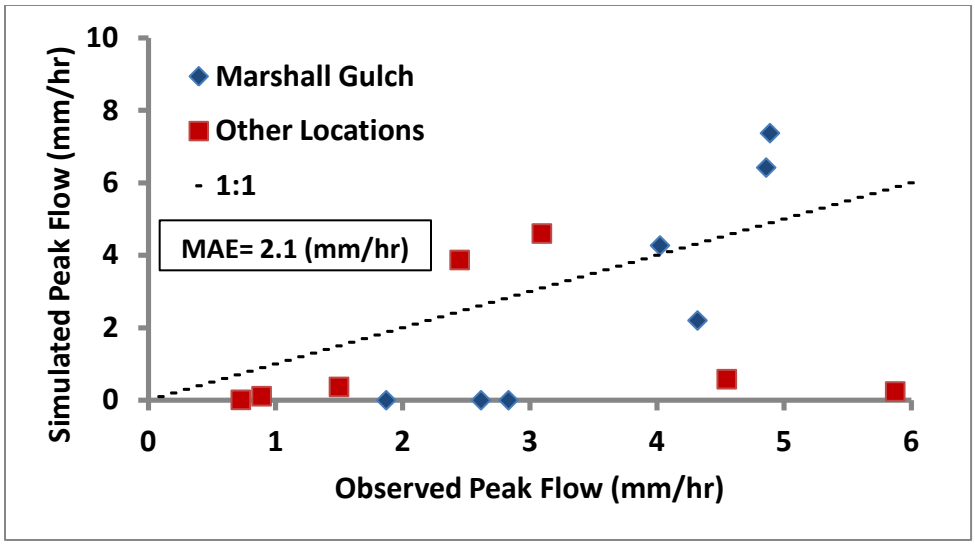

Figure 26. Comparison of simulated and observed peak flow rates using default cover estimates and global multipliers to account for rainfall intensity (Equation 2).

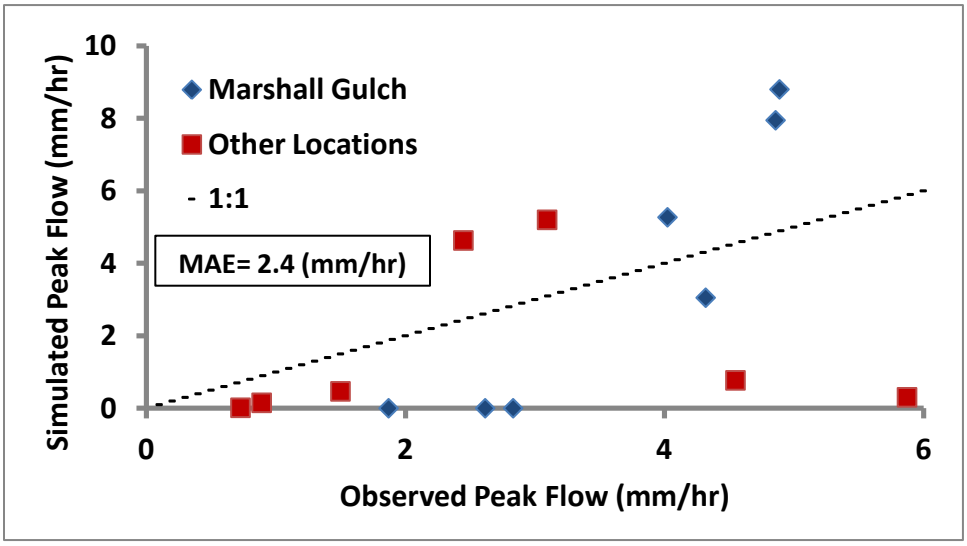

Figure 27. Comparison of simulated and observed peak flow rates using remotely sensed cover estimates and global multipliers to account for rainfall intensity (Equation 2).

Figures 28 and 29 show selected modeling results incorporating the rainfall intensity relation and calibrations made for burned areas on both the default AGWA land cover and for the remotely sensed land cover scenarios. In both of these cases the Ks and Manning's *n* parameter values had a multiplier of 0.9 applied in burned modeling elements. Results shown in Figure 28 for the AGWA default land cover yielded an MAE of 2.4 indicating that altering burned area parameter estimates did not improve modeling results. The modeling results for the remotely sensed land cover scenario (Figure 29) yielded an MAE of 2.7 indicating that neither the alternative land cover nor the reductions to burned area parameter values made improvements to peak flow rate estimates.

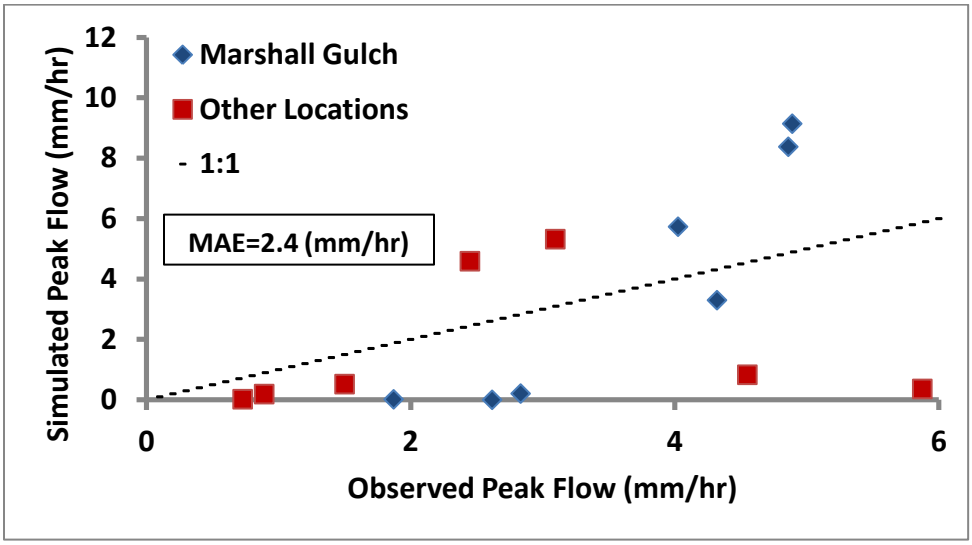

Figure 28. Comparison of observed and simulated predictions of peak flow rates using AGWA (NLCD) estimates of cover. This is showing results for a simulation that considered the Ks_{ap} : I30 relation and also applied calibrating multipliers of 0.9 to Ks, and 0.9 to Manning's *n*.

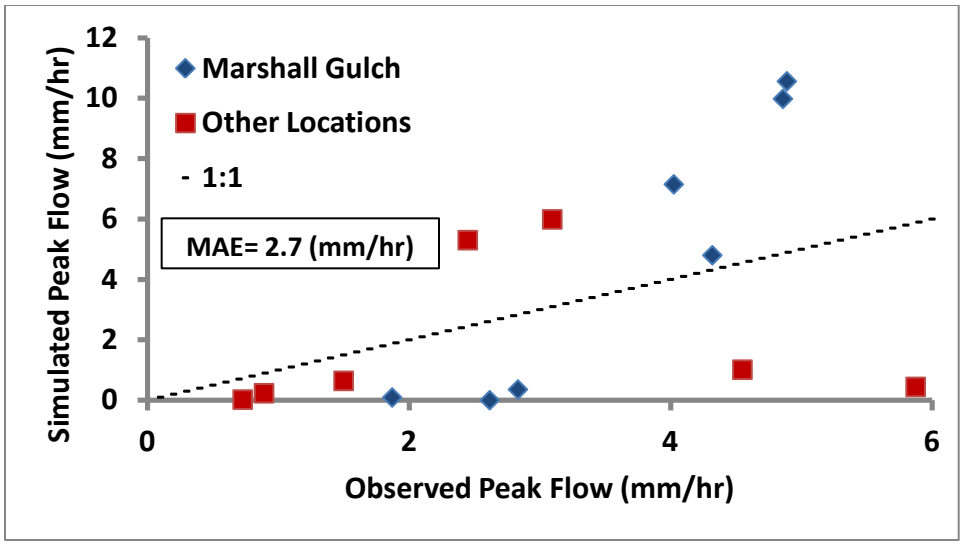

Figure 29. Comparison of observed and simulated predictions of peak flow rates using remotely sensing based estimates of cover. This figure is showing results for a simulation that considers the Ks_{ap} : I30 relation and also applied calibrating multipliers of 0.9 to Ks, and 0.9 to Manning's *n*.

Modeling results shown in the one to one comparisons of peak flow rates in Figures 24-29 and in Table 11 indicate that reduction of burned area parameter values and the remotely sensed land cover values did not improve modeling results. However, accounting for rainfall intensity improved modeled peak flow rates substantially.

4.7 Comparing Modeled Percent Change to Observed Storm Percent Change at Marshall Gulch

To test how well the relative change approach captures the degree of change that happens after a fire, uncalibrated simulated peak flows for burned and unburned conditions were compared to observed peak flows in burned and unburned conditions at Marshall Gulch (Figures 30-33). Figure 30 shows the hyetograph for the five year one hour design storm used to drive these uncalibrated simulations and the hydrographic

response for burned and unburned conditions and Figure 31 shows the uncalibrated pre and post-fire simulations driven by the natural storm of 7/24/2003. The storms represented in the hyetographs in Figures 32-33 were chosen for their similarity in rainfall accumulation and intensity and duration to each other and to the five year one hour design storm. The five year one hour return period NOAA design storm was disaggregated into 12 steps to generate a comparable I30. The storm of 7/27/2013 was chosen to represent the "unburned recovered" condition. Using the recovered watershed conditions to represent the unburned condition was reasonably justified in section 4.2. Table 12 summarizes simulated and observed peak flow rates and percent change for pre-fire and post-fire conditions.

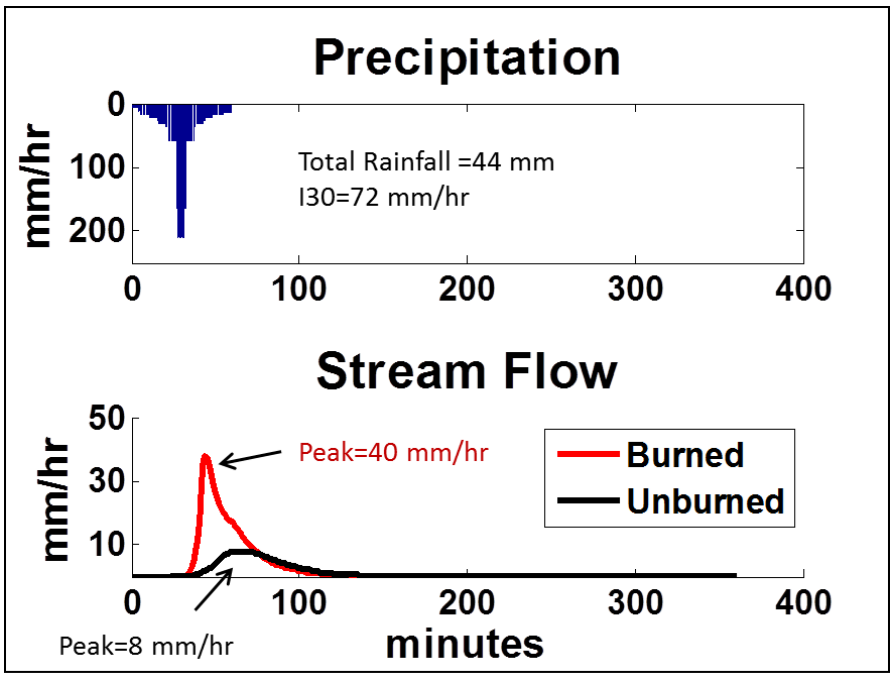

Figure 30. Relative difference for uncalibated model runs at Marshall Gulch. Using a 5 year 1 hour design storm represented with 12 time intervals to drive the model in unburned and burned conditions a percent change of 381% was determined.

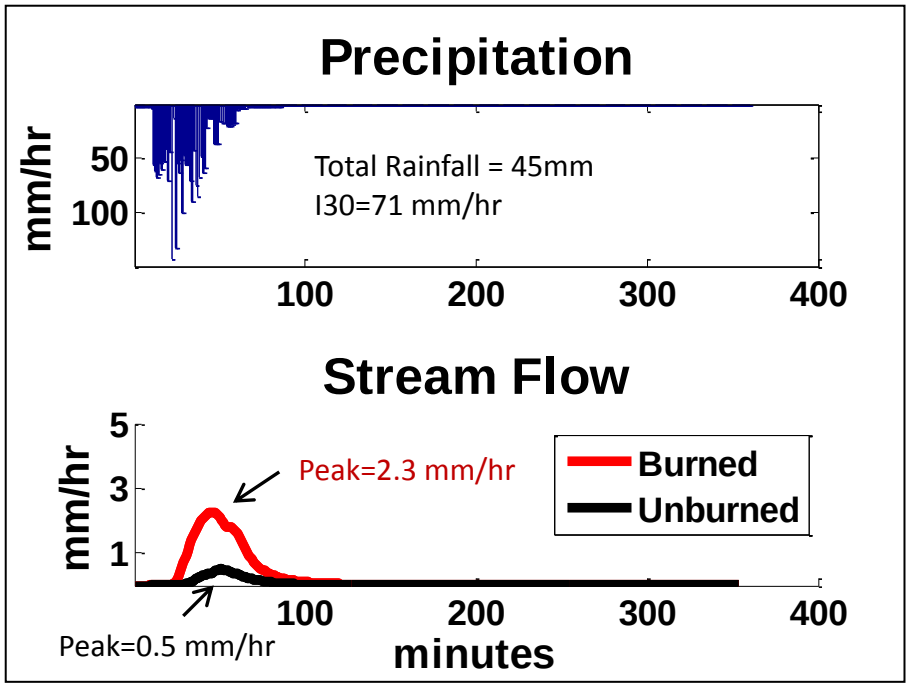

Figure 31. Relative difference for uncalibated model runs at Marshall Gulch. Using the storm of 7/24/2003 to drive the model in unburned and burned conditions a percent change of 360% was determined.

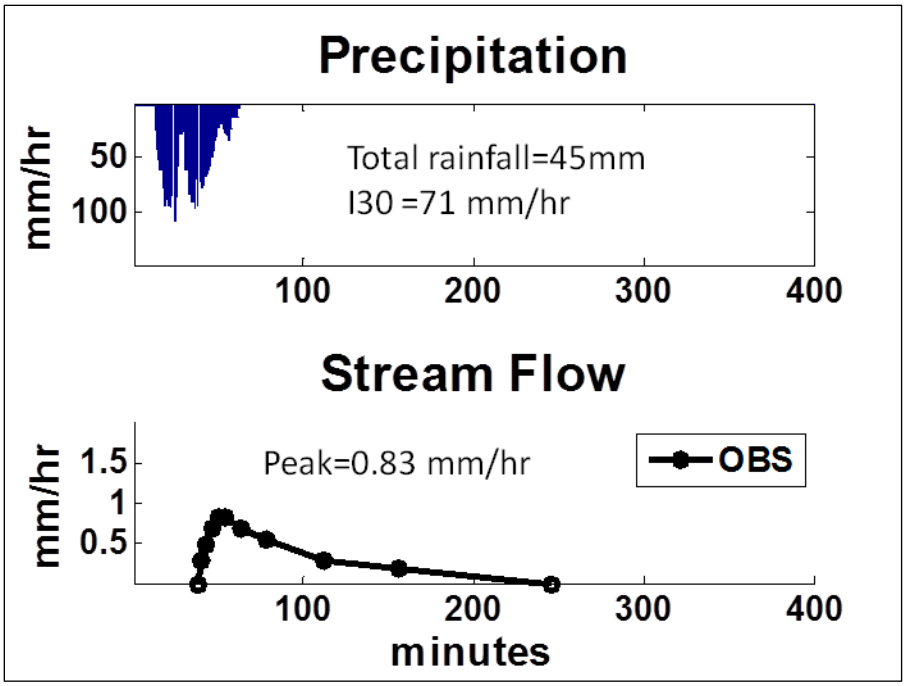

Figure 32. Storm of 7/27/2013 at Marshall Gulch. This figure shows the storm hyetograph and hydrograph data collected in the unburned (assumed to be recovered) condition.

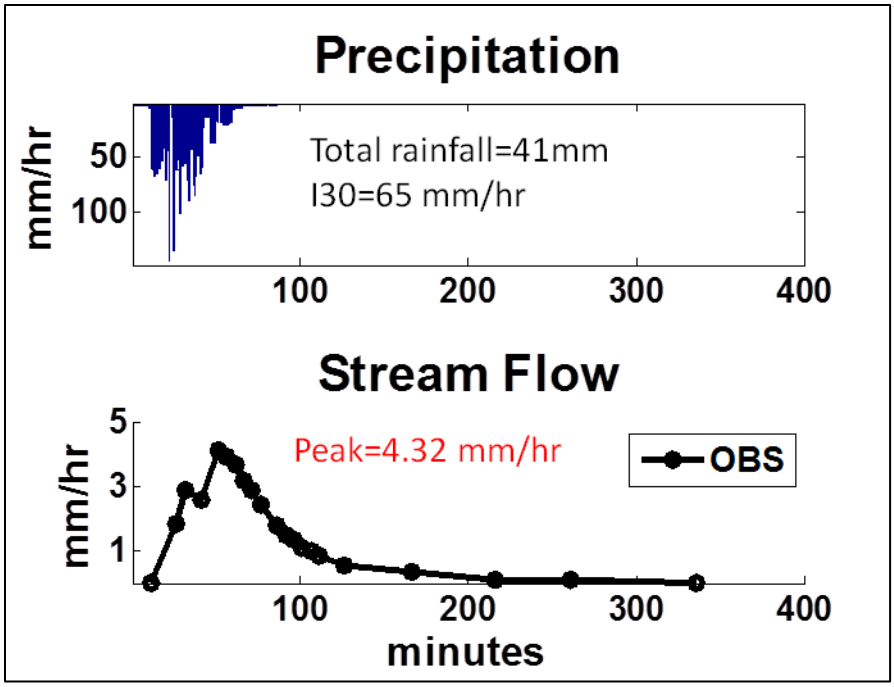

Figure 33. Storm of 7/24/2003 at Marshall Gulch. This figure shows the storm hyetograph and hydrograph data collected in the burned condition.

Table 12. Peak flow rates and percent change for pre and post-fire AGWA simulations using a design storm and a natural storm. Peak flow rates and percent change for observed natural (1957) and burned conditions (2003), recovered forest (2013) and burned conditions (2003) and natural (1957) and recovered forest (2013) conditions.

Peak flow rate (mm/hr)	**AGWA pre-fire : post-fire 5 year 1 hour design storm**	**AGWA pre-fire : post-fire using rainstorm of 7/24/2003**	**Natural (8/16/1957) : Burned (7/24/2003)[1]**	**Recovered (7/27/2013) : Burned (7/24/2003)**	**Natural (8/16/1957) : Recovered (7/27/2013)**
Pre	7.9	0.5	0.16	0.83	0.16
Post	38	2.3	4.14	4.14	0.83
% Change	**381**	**360**	**2488**	**420**	**419**

[1] See Figure 1.

The results shown in Table 12 indicate that the AGWA modeling scheme as it currently exists predicts a change in peak flow rate due to wildfire that is quite close to the change in peak flow rates observed for burned and recovered conditions. Uncalibrated model runs using a natural storm also had a similar percent change. The difference is also quite similar to the change between the peak flow rates observed in the recovered and natural conditions, possibly indicating that a full recovery to natural conditions has not occurred. The difference in peak flow rates observed in the recovered and natural condition likely has more to do with the degree of ground cover present than the canopy cover. The percent change in peak flow rates observed for natural conditions and post-fire conditions is an order of magnitude greater than the simulations or the recovered vs. burned scenario. This provides an idea of the range of possible increases to peak flow rates. The temporal nature of the rainstorm that fell on the natural condition is

not known as the rainfall accumulation was reported on the daily time step, so the storms may not be as comparable as the storms of 7/27/2013 and 7/24/2003.

Further investigation was made into the percent change approach using the five year one hour NOAA design storm disaggregated into 6, 8, 12, and 16 time steps and the natural storms of 7/24/2003 and 7/27/2013 to drive simulations parameterized by the current AGWA LUT, parameter estimations based on remotely sensed canopy cover values, parameter estimations taking Ks_{ap} into account (via Eq. 2), and parameter estimations using remote sensing and accounting for the Ks_{ap}. Results for this analysis are shown in Table 14. Characteristics for rainstorms used in this analysis are shown in Table 13. Hyetographs for the NOAA five year one hour SCS type II design storms are shown in Figure 34, and hyetographs for the natural storms of 7/24/2003 and 7/27/2013 are shown in Figure 35.

Table 13. Characteristics for rainstorms used in percent change analysis.

Rainstorm	**NOAA 5 year 1 hour design storm**				**Natural**	
	6 time step SCS II storm	8 time step SCS II storm	12 time step SCS II storm	16 time step SCS II storm	7/24/2003	7/27/2013
Rainfall accumulation (mm)	44	44	44	44	41	45
Peak rainfall intensity (mm/hr)	132	161	210	242	143	110
Peak 30 minute rainfall intensity (I30) (mm/hr)	70.2	71.4	71.7	71.8	64.7	70.8

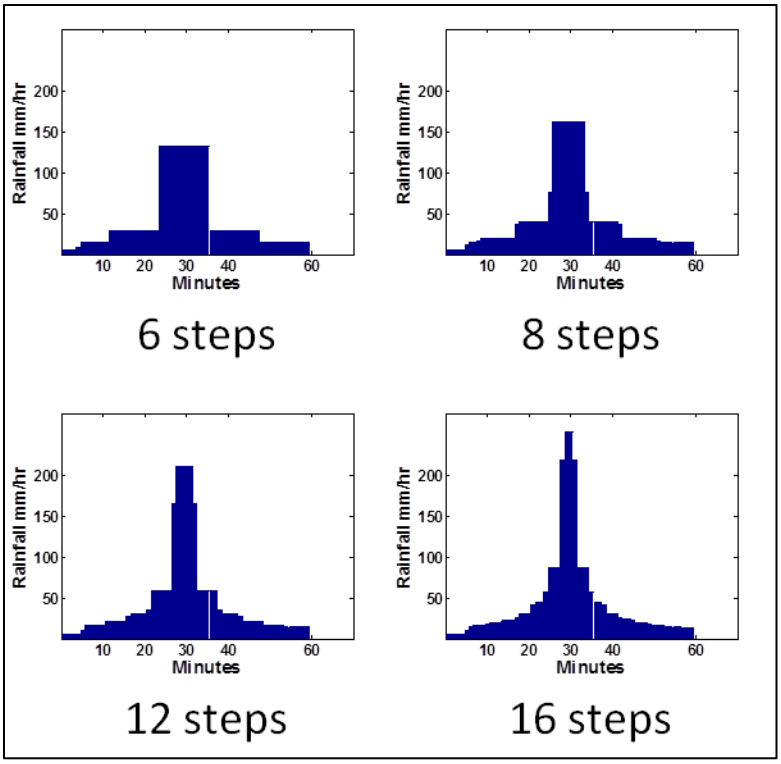

Figure 34. Hyetographs for NOAA 5 year 1 hour SCS II design storms disaggregated into 6, 8, 12 and 16 time steps.

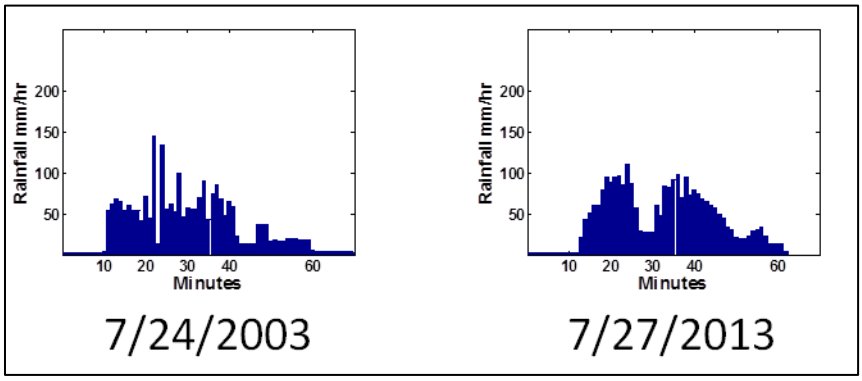

Figure 35. Hyetographs for natural storms recorded at Marshall Gulch on 7/24/2003 and 7/27/2013.

Table 14. Percent change analysis for the current AGWA scheme and the proposed alterations to the AWGA scheme using remotely sensed canopy cover and accounting for apparent infiltration rates (Ks_{ap}) and the combination of Ks_{ap} and remotely sensed values of canopy cover. Simulations were driven by NOAA 5 year 1 hour SCS II design storms disaggregated into 6, 8, 12 and 16 time steps, and the natural storms recorded on 7/24/2003 and 7/27/2013.

Rain storms	**NOAA 5 year 1 hour design storm**				**Natural**	
	5 year 1 hour 6 steps	5 year 1 hour 8 steps	5 year 1 hour 12 steps	5 year 1 hour 16 steps	7/24/2003	7/27/2013
AGWA LUT canopy cover values						
Pre-fire peak flow (mm/hr)	7.6	7.8	7.9	8.0	6.8	11.0
Post-fire peak flow (mm/hr)	33.0	35.0	38.0	38.8	20.0	30.0
Percent Change	**334**	**349**	**381**	**385**	**194**	**173**
Remotely Sensed canopy cover values						
Pre-fire peak flow (mm/hr)	6.3	6.5	6.6	6.8	5.9	9.7
Post-fire peak flow (mm/hr)	34	36.6	39	39.8	13.3	19.2
Percent Change	**440**	**463**	**491**	**485**	**125**	**98**
AGWA LUT canopy cover values accounting for Ks_{ap}						
Pre-fire peak flow (mm/hr)	0.075	0.13	0.28	0.31	0.51	0.008
Post-fire peak flow (mm/hr)	9.75	11.7	14.0	14.8	2.3	6.4
Percent Change	**12660**	**9064**	**4929**	**4656**	**353**	**79400**
Remotely Sensed canopy cover values accounting for Ks_{ap}						
Pre-fire peak flow (mm/hr)	0.025	0.04	0.12	0.15	0.20	0.0004
Post-fire peak flow (mm/hr)	11.6	13.9	16.2	16.9	3.1	8.0
Percent Change	**46140**	**34575**	**13425**	**11496**	**1450**	**2007400**

The results shown in Table 14 show that the number of time steps that an SCS type II design storm is disaggregated into has an effect on modeling results. This has to do with how rainfall intensity is distributed in time, as seen in Figure 31. For the AGAW LUT parameter simulations and the remotely sensed canopy cover simulations the natural storms produced lower percent changes than the design storms. This is likely due to the fact that the natural storms were applied in a spatially distributed manner as interpolated based on three raingages where the design storms applied rainfall uniformly to the entire watershed, meaning that slightly more rainfall was likely applied for the design storms. The portion of the analysis that takes into account the Ks_{ap} shows pre-fire peak flow values that are close to the observed values for flows recorded in the natural and recovered conditions, and post-fire peak flow rates that are closer to observed than those generated by simulations that did not take the Ks_{ap} into consideration. However, the prediction for percent change for peak flow rate seems to be relatively poor for all storms except for the natural event of 7/24/2003. Using a temporally and spatially dynamic multiplier to account for rainfall intensity effects would be more appropriate than the static approach taken here, and could likely improve modeling results. This will be discussed further in section 5.4.

The differences in percent change calculated for peak flow rates for the remotely sensed parameter estimates are slightly larger than the percent changes calculated using the AGWA parameter estimate scheme as it is. With both of these schemes estimating realistic percent changes, the remotely sensed estimation could be adopted as a more conservative estimate of change. Most notably the percent cover estimate for severely burned coniferous forest should be changed from 25% to 10% (Table 7). Further

investigation into the use of remotely sensed cover values will be discussed in section 5.3 in more detail.

Spearman's rank correlation coefficient as outlined in McBean and Rovers (1998) was used to determine how the ranking of the percent change changed per modeling element based on the storm used or the parameter estimation scheme used. Results from these tests are shown in Tables 15 and 16 respectively. Simulations shown in Table 16 were driven by the NOAA five year one hour SCS type II design storms and the natural storm of 7/24/2003.

Table 15. Spearman's rank correlation for percent change in peak flow results in modeling elements for NOAA 5 year 1 hour SCS II design storms at Marshall Gulch (disaggregated into 8, 12 and 16 time steps) and the natural storm recorded on 7/24/2003.

Percent change in peak runoff from hillslope modeling elements			
8 step SCS II	0.99	0.99	0.93
1.00	12 step SCS II	0.99	0.92
1.00	1.00	16 step SCS II	0.93
0.99	0.99	0.99	Natural 7/24/2003
Percent change in peak flow from channel elements			

Table 16. Spearman's rank correlation for percent change in peak flow results in modeling elements for the parameter estimation schemes tested. AGWA represents the AGWA scheme as it exists currently, RS represents the remotely sensed estimates of canopy cover, AGWA + Ks_{ap} represents the scheme that incorporates apparent infiltration rates with AGWA LUT values for canopy cover, and RS + Ks_{ap} represents the scheme that incorporates apparent infiltration rates with remotely sensed canopy cover values.

Percent change in peak runoff form hillslope modeling elements			
AGWA	1.00	0.99	0.99
1.00	RS	0.99	0.99
0.97	0.97	AGWA + Ks_{ap}	0.93
0.97	0.97	1.00	RS + Ks_{ap}
Percent change in peak flow from channel elements			

The investigation into the correlation of the rankings of percent change indicate that results for all storms used, and for the differing parameter estimation schemes, the rankings are all strongly correlated if not identical. This result indicates that the risk assigned to any of the modeling elements by a BAER team would be the nearly the same no matter how rainfall was applied or which parameter estimation scheme was used.

5. FINDINGS

5.1 Assessment of Remotely Sensed Estimates of Canopy Cover

Remote sensing was successfully used as a part of this study. Insights were gained for the duration of a hydrologic recovery period following the Aspen Fire that occurred in Marshall Gulch. It was sufficiently illustrated through the use of the maximum annual NDVI that by ten years following the fire that the deciduous vegetation had returned to pre-fire levels. This allowed for a portion of the recorded data for rainfall

and stream flow be categorized to represent the unburned condition. This proved useful for the assessment of the relative change approach used by BAER teams. Remote sensing also was used to provide estimations of cover for unburned as well as low, moderate, and high degrees of burn for the coniferous/evergreen land cover category. These estimates were quite close to the estimates provided by AGWA LUT for all categories except for high burn severity. The high burn severity category was remotely sensed to have a 10% cover value where the AGWA LUTs estimate 25%. Although this change was not shown to improve modeled peak flow results, it could be incorporated into the AGWA LUTs as a more conservative estimate of percent change.

5.2 Assessment of KINEROS2 Calibrations

The KINEROS2 model was calibrated focusing on data collected at Marshall Gulch. This location had the longest record of data that included the most post-fire storm events. The rainfall intensity of the observed storms varied dramatically, as did the calibrated parameters for infiltration. This demonstrated that for a study where infiltration rates are to be determined by calibration based on outflow measurements observed at the outlet of a watershed, the apparent infiltration rate must be taken into consideration. Calibration efforts were a success in terms of revealing a significant correlation between rainfall intensity and calibrated infiltration rates using an artificially lumped "uniform cover" scenario, however no improvements to burned area parameter values for Manning's *n* or Ks were revealed when using the "burned" land cover scenario.

5.3 Testing Parameters Developed at Marshall Gulch at Other Burned Locations in New Mexico and Colorado

Tests of calibrated parameter values included burned watersheds in New Mexico and Colorado. These tests revealed that adjustments made to the Ks parameter to account for the apparent infiltration rate as determined at Marshall Gulch did improve modeling results for peak flow rates. This association of rainfall intensity to the apparent infiltration rate is a proxy used to better model deep overland flow depths, and therefore higher infiltration rates (Dunne et al., 1991), that occur during high rainfall intensity events. Neither changes to burned area parameter values nor the use of remotely sensed land cover values further improved estimates of peak flow rates.

5.4 Comparing Current AGWA Procedures for BAER to Observed Data

Interesting results were found when assessing the percent change approach that is used for rapid post-fire assessment. Using results for peak flow rates generated by model runs driven by a NOAA SCS type II design storm and the natural storm that occurred in Marshall Gulch on 7/24/2003, the AGWA/KINEROS2 scheme as it currently exists predicted a percent change very close to what was observed in Marshall Gulch for a comparable set of storms. When considering adjustments to the Ks parameter based on rainfall intensity, the predicted values of peak flow rates were closer to the observed in both the unburned and burned conditions, but the percent change was much greater than observed. Of all the different rainstorms and parameter estimation schemes compared for differences in percent change, no model results produced substantial changes to the rankings for the degree of change that occurred in the modeling elements.

5.5 No Justification for Burned Area Parameter Adjustments

There are many factors that challenged this study: the spatial variability of burn patterns that occurred in these watersheds, the inherent uniqueness of each watershed, differing characteristics of the rainfall that was recorded at each of the watersheds (spatial, temporal and intensity) and the recognition that the information recorded for rainfall and runoff may have been subject to high uncertainty. The Marshall Gulch data set for runoff which was intensely used in this study relied on an extrapolated rating curve to characterize large post-fire flood events. It is unlikely that a burned watershed will have a relevant stream flow gage to use for model calibration, and as was the case with Marshall Gulch, it is also unlikely that post-fire flood levels would be included in a depth-discharge rating curve. Additional limitations such as a non-comprehensive representation of runoff generation and the potential for over generalization when abstracting real conditions into modeling elements are inherent to the AGWA/KINEROS2 modeling scheme.

Considering the challenges and limitations inherent to this study, it is concluded that changes to the AGWA parameter assignment scheme for burned areas is not warranted at this time. It is the belief of the author that adjustments to hillslope parameters are not justifiable by a modeling exercise that only compares modeled results to measured results at the watershed scale. Due to the heterogeneous nature of the hillslopes that compose a watershed, even without the heterogeneous distribution of disturbance created by fire, it is not possible to identify hillslope characteristics simply by the amount of water that reaches the catchments outlet. Stream flow generation

mechanisms and rainfall patterns that are not well characterized make parameter estimation based on runoff measurements at the watershed scale unadvisable.

6. FUTURE WORK

6.1 Limitations and Recommendations for Further Research

This study was primarily a modeling exercise. None of the sites were physically observed post-fire. Limited observations were made at the Marshall Gulch location nearly a decade after the fire, and were focused on stream channel roughness. Field observations made at a time closer to when the fire was extinguished at all of the test basins could have had a profound impact on the parameter assignment decisions.

Instead of the approach taken here with records of runoff and rainfall from gaged watersheds it is suggested that a more experimental approach be taken to generate better burned area parameter estimates for the AGWA parameter estimation scheme. The proposed experiment would limit the spatial scale of the study area to the plot scale where the spatial variability of the burn severity would be limited to only one category, low, moderate or severe. This would not only limit the heterogeneity of the burn intensity, but it would also limit the spatial variability that existed in the unburned condition. The plot scale would also make the experiment appropriate for rainfall simulation input. This would have several advantages. By simulating the rainfall input there would be a much greater potential for data collection. The damaging rainstorms that are of concern are not necessarily going to naturally occur during the time that the burned landscape is the most at risk, or in watersheds that happen to have been instrumented. By controlling the intensity rate of the simulated rainfall, better

information about how infiltration rates vary with intensity could be investigated specifically in the context of the burned area and its micro-topography. And finally, there would be no question as to the spatial extent of the rainfall, and if it was captured by the instrumentation. A known amount of water would be put into the system, and a known amount could be gathered at the outlet of the plot as well.

Further research should also be conducted for remotely sensed canopy cover values of burned watersheds. Although the remotely sensed values of canopy cover at Marshall Gulch showed some difference for the severely burned category of evergreen forest, the remaining categories of forest cover were quite similar. More research should be done to show that this is not a coincidence or to develop a more robust estimate of canopy cover based on observances at many watersheds.

6.2 Improvements to AGWA/KINEROS2

Given that KINEROS2 only generates runoff by infiltration excess it makes a certain degree of sense that rainfall intensity is the primary influencing factor. The apparent infiltration rate emphasizes the importance of rainfall intensity as was seen by the observations of Dunne et al. (1991) and Stone et al. (2008) where the apparent infiltration rates changes as a function of runoff depth which is related to rainfall intensity in an infiltration excess runoff regime.

Currently, the scheme in which KINEROS2 partitions rainfall into infiltrated water, and runoff is being reconfigured to account for shallow sub-surface storm flow. KINEROS2 also has the ability to account for a two layered soil system of varying depth and Ks, which could potentially account for saturation excess runoff generation. These

improvements once incorporated into the AGWA interface, will make the modeling scheme more suitable for forest conditions. This may allow for better calibration attempts at burned watersheds and may make its use for post-fire risk assessment better but would also require additional soils information across the watershed.

This research inspired the ability to apply calibrating multipliers to specific modeling elements in KINEROS2 as opposed to all modeling elements. The intent was to only alter modeling elements that had been burned, but this functionality could be useful in other scenarios. The scheme used in this thesis to account for Ks_{ap} was limited in that multipliers were applied to infiltration rates for the entire watershed for the entire duration of the storm. This was regardless of if rainfall was falling intensely during a particular time in the storm or not, or if rain was falling intensely on a particular part of the watershed or not. If functionality is built into KINEROS2 to adjust infiltration rates based on the time and place that rain was falling intensely on a watershed, a better investigation into how to apply intensity variant infiltration rates to a watershed could be conducted. Or better yet, once the ability to characterize hillslope microtopography better is realized, flow depth variant infiltration rates (for which Ks_{ap} is a surrogate) could be incorporated into the KINEROS2 model.

APPENDIX A- NDVI BASED CONIFEROUS FOREST CANOPY COVER ESTIMATES

Six sample regions were defined in old growth stands within the Andrews Experimental Forest (Figure 1a). NDVI values were calculated from all available Landsat 5 TM CDR surface reflectance images from 1/1/2002 – 1/1/2012. Maximum NDVI values were extracted from each sample region for the time series {Min_Max_NDVI.xls}. The median value for the time series of each sample location was then determined to eliminate any anomalies. The maximum of these median NDVI values, 0.91, was assumed to be representative of 100% coniferous forest canopy cover.

Figure 1a. Sample locations (blue) with Andrews Experimental Forest (white).

To determine the minimum NDVI (bare soil) value, Landsat 5 TM images were acquired for the Marshall Gulch region from 1/1/2002 – 1/1/2012. Only cloud free images from June – September were selected for the time series to ensure the absence of snow. The minimum NDVI value from this series, 0.11, was selected as the 0% (bare soil) canopy cover value.

Landsat 5 TM CDR surface reflectance images were acquired though USGS Earth Explorer for image dates: 5/15/2003, 6/16/2003, 7/2/2003, 9/4/2003 and Normalized Difference Vegetation Index (NDVI) values were calculated for each image (Equation 1) {YYYY_MM_DD_NDVI.tiff – WGS84 Zone 12}.

$$NDVI = \frac{\rho_{NIR} - \rho_{RED}}{\rho_{NIR} + \rho_{RED}} \qquad \rho = Surface\ Reflectance \quad (Equation\ 1a)$$

Canopy cover (%) values for the images were calculated using the two NDVI end members ($NDVI_{MIN}$ and $NDVI_{MAX}$) in a simple linear mixture model (Equation 2a) {YYYY_MM_DD_NDVI.tiff - WGS84 Zone 12}.

$$Canopy\ Cover\ \% = \frac{NDVI_{i,j} - NDVI_{MIN}}{NDVI_{MAX} + NDVI_{MIN}} \times 100\% \quad NDVI_{i,j} = pixel(i,j) \quad (Equation\ 2a)$$

$$Canopy\ Cover\ \% = \frac{NDVI_{i,j} - 0.11}{0.79} \times 100\% \quad (Equation\ 3a)$$

REFERENCES

Abrahams, A. D., Parsons, A. J., & Wainwright, J. (1995). Effects of vegetation change on interrill runoff and erosion, Walnut Gulch, southern Arizona. *Geomorphology*, *13*(1), 37-48.

Anderson, H. W., Hoover, M. D., & Reinhart, K. G. (1976). Forests and water: effects of forest management on floods, sedimentation, and water supply. USDA Forest Service Technical Report PSW- 18/1976, Pacific Southwest Forest and Range Experiment Station.

Bhark, E. W., & Small, E. E. (2003). Association between plant canopies and the spatial patterns of infiltration in shrubland and grassland of the Chihuahuan Desert, New Mexico. *Ecosystems*, *6*(2), 185-196.

Bobbe, T., Finco, M., Maus, P., & Orlemann, A. (2001). Remote Sensing Tools for Burned Area Emergency Rehabilitation (BAER). USDA Forest Service, Remote Sensing Applications Center. RSAC-1-TIP1.

Bulygina, N. S., Nearing, M. A., Stone J. J., & Nichols, M. H. 2007. DWEPP: a dynamic soil erosion model based on WEPP source terms. Earth Surface Processes and Landforms. DOI: 10.1002/esp.1467.

Burns, I.S., Korgaonkar, Y., Guertin, D. P., Goodrich, D.C., Kepner, W. A., Miller S. N. & Semmens D. J. (2013). *Automated Geospatial Watershed Assessment (AGWA) 3.0 Software Tool*. Washington, DC: USDA Agricultural Research Service and U.S. EPA. Retrieved from http://www.tucson.ars.ag.gov/agwa/.

Canfield, H.E., Goodrich, D. C., & Burns, I. S. (2005). Application of models to predict post-fire runoff and sediment transport at the watershed scale in southwestern forests. In *Proc. Amer. Soc. Civil Engr. 2005 Watershed Management Conference, July 22-25, Williamsburg, VA*, 12p., CD-ROM.

Cerdá, A., & Doerr, S. H. (2005). Influence of vegetation recovery on soil hydrology and erodibility following fire: an 11-year investigation. *International Journal of Wildland Fire*, *14*(4), 423-437.

Chen, L., Berli, M., & Chief, K. (2013). Examining Modeling Approaches for the Rainfall-Runoff Process in Wildfire-Affected Watersheds: Using San Dimas Experimental Forest. *Journal of the American Water Resources Association*, *49*(4), 851-866.

Chow, T. V. (1959). Open channel hydraulics. New York, NY: McGraw-Hill.

Cowan, W. L. (1956). Estimating hydraulic roughness coefficients. *Agricultural Engineering*, *37*(7), 473-475.

D'Alonzo, K. T. (2004). The Johnson-Neyman procedure as an alternative to ANCOVA. *Western Journal of Nursing Research*, *26*(7), 804-812.

DeBano, L. F., Ffolliott, P. F., & Baker Jr, M. B. (1996). Fire severity effects on water resources. In *Proc. Symposium on Effects of Fire on Madrean Province Ecosystems, March 1996, Tucson, AZ.*

DeBano, L. F., Neary, D. G., & Ffolliott, P. F. (1998). Fire effects on ecosystems. Hoboken, NJ: John Wiley & Sons.

DeBano, L. F. (2003). The role of fire and soil heating on water repellency. *Soil water repellency: occurrence, consequences and amelioration*, 193-202. Ritsema, C. J., & Dekker, L. W. (Ed.). Amsterdam: Elsevier Science

Dunne, T., Zhang, W., & Aubry, B. F. (1991). Effects of rainfall, vegetation, and microtopography on infiltration and runoff. *Water Resources Research*, *27*(9), 2271-2285.

Faurès, J. M., Goodrich, D. C., Woolhiser, D. A., & Sorooshian, S. (1995). Impact of small-scale spatial rainfall variability on runoff modeling. *Journal of Hydrology*, *173*(1), 309-326.

Gassman, P. W., Reyes, M. R., Green, C. H., & Arnold, J. G. (2007). The soil and water assessment tool: historical development, applications, and future research directions. *Transactions of the ASABE*, *50*(4), 1211-1250.

Gómez, J. A., Giráldez, J. V., & Fereres, E. (2001). Analysis of infiltration and runoff in an olive orchard under no-till. *Soil Science Society of America Journal*, *65*(2), 291-299.

Goodrich, D. C., Canfield, H. E., Burns, I. S., Semmens, D. J., Miller, S. N., Hernandez, M., & Kepner, W. G. (2005). Rapid post-fire hydrologic watershed assessment using the AGWA GIS-based hydrologic modeling tool. In *Proc. ASCE Watershed Manage. Conf., July* (pp. 19-22).

Goodrich, D. C., Burns, I. S., Unkrich, C. L., Semmens, D. J., Guertin, D. P., Hernandez, M., & Levick, L. R. (2012). KINEROS2/AGWA: Model use, calibration, and validation. *Transactions of the ASABE*, *55*(4), 1561-1574.

Gupta, H. V., Kling, H., Yilmaz, K. K., & Martinez, G. F. (2009). Decomposition of the mean squared error and NSE performance criteria: Implications for improving hydrological modelling. *Journal of Hydrology*, *377*(1), 80-91.

Hawkins, R. H. (1982). Interpretations of source area variability in rainfall-runoff relations. In V. P. Singh (Ed.), *Rainfall-Runoff Relationship* (pp.303-324). Littleton, CO: Water Resources Publications

Hernandez, M., Miller, S. N., Goodrich, D. C., Goff, B. F., Kepner, W. G., Edmonds, C. M., & Jones, K. B. (2000). Modeling runoff response to land cover and rainfall spatial variability in semi-arid watersheds. In *Monitoring Ecological Condition in the Western United States* (pp. 285-298). Springer Netherlands.

Holden, J., & Burt, T. P. (2002). Infiltration, runoff and sediment production in blanket peat catchments: implications of field rainfall simulation experiments. *Hydrological Processes*, *16*(13), 2537-2557.

Hossain, F., Anagnostou, E. N., Dinku, T., & Borga, M. (2004). Hydrological model sensitivity to parameter and radar rainfall estimation uncertainty. *Hydrological Processes*, *18*(17), 3277-3291.

Janeau, J. L., Mauchamp, A., & Tarin, G. (1999). The soil surface characteristics of vegetation stripes in Northern Mexico and their influences on the system hydrodynamics: An experimental approach. *Catena*, *37*(1), 165-173.

Kinner, D. A., & Moody, J. A. (2008). Infiltration and runoff measurements on steep burned hillslopes using a rainfall simulator with variable rain intensities. U.S. Geological Survey Report No. 2007-5211.

Kinoshita, A. M., Hogue, T. S., & Napper, C. (2014). Evaluating Pre-and Post-Fire Peak Discharge Predictions across Western US Watersheds. *Journal of the American Water Resources Association*, *50*(6), 1540-1557.

Lane, L. J., Gilley, J. E., Nearing, M., & Nicks, A. D. (1989). The USDA Water Erosion Prediction Project. In *Hydraulic Engineering* (pp. 391-396). ASCE.

Lentile, L. B., Morgan, P., Hudak, A. T., Bobbitt, M. J., Lewis, S. A., Smith, A. M. S., & Robichaud, P. R. (2007). Post-fire burn severity and vegetation response following eight large wildfires across the western United States. *Fire Ecology Special Issue*, *3*(1), 91-108.

McBean, E. A, & Rovers, F. A. (1998). Statistical procedures for analysis of enviromental monitoring data and assessment. Upper Saddle River, NJ: Prentice Hall.

Meixner, T., & Wohlgemuth, P. (2004). Wildfire Impacts on Water Quality. *Journal of Wildland Fire*, *13*(1), 27-35.

Miller, S. N., Semmens, D. J., Goodrich, D. C., Hernandez, M., Miller, R. C., Kepner, W. G., & Guertin, D. P. (2007). The automated geospatial watershed assessment tool. *Environmental Modelling & Software*, *22*(3), 365-377.

Moody, J. A. (2011). An analytical method for predicting postwildfire peak discharges. *US Geological Survey Scientific Investigations Report*, *5236*(2012), 36.

Morin, J., & Kosovsky, A. (1995). The surface infiltration model. *Journal of Soil and Water Conservation*, *50*(5), 470.

Morin, E., Goodrich, D. C., Maddox, R. A., Gao, X., Gupta, H. V., & Sorooshian, S. (2006). Spatial patterns in thunderstorm rainfall events and their coupling with watershed hydrological response. *Advances in Water Resources*, *29*(6), 843-860.

Napper, C., (2010). BAER Hydrology Model Questionnaire Results. USDA, Forest Service Technology and Development Center, San Dimas, California.

Nash, J. E., & Sutcliffe, J. V. (1970). River flow forecasting through conceptual models part I—A discussion of principles. *Journal of Hydrology*,*10*(3), 282-290.

National Oceanic and Atmospheric Administration (2013) *NOAA Atlas 14 Point Precipitation Frequency Estimates*. Retrieved from http://hdsc.nws.noaa.gov/hdsc/pfds/pfds_map_cont.html?bkmrk=nm

Natural Resources Conservation Service (2014) *Soil Data Access*. Retrieved from http://www.sdmdataaccess.nrcs.usda.gov

National Climatic Data Center (2014) NOAA *National Climatic Data Center*. Retrieved from http://www.ncdc.noaa.gov/nexrading/map.jsp

Nearing, M. A., Wei, H., Stone, J. J., Pierson, F. B., Spaeth, K. E., Weltz, M. A. & Hernandez, M. (2011). A rangeland hydrology and erosion model. *Transactions of the ASABE*, *54*(3), 901-908.

Paige, G. B., Stone, J. J., Guertin, D. P., & Lane, L. J. (2002).). A strip model approach to parameterize a coupled Green-Ampt kinematic wave model. . *Journal of the American Water Resources Association*, *38*(5), 1363-1377.

Phillips, J. V., & Tadayon, S. (2006). Selection of Manning's roughness coefficient for natural and constructed vegetated and non-vegetated channels, and vegetation maintenance plan guidelines for vegetated channels in Central Arizona. U.S. Geological Survey Report No. 2006-5108.

Rawls, W. J., Brakensiek, D. L., & Saxtonn, K. E. (1982). Estimation of soil water properties. *Transactions of the ASAE*, *25*(5), 1316-1320.

Robichaud, P. R., Beyers, J. L., & Neary, D. G. (2000). Evaluating the effectiveness of postfire rehabilitation treatments, General Technical Report RMRS-GTR-63, US

Department of Agriculture, Forest Service, Rocky Mountain Research Station Fort Collins, CO, USA.

Robichaud, P. R., Lewis, S. A., Wagenbrenner, J. W., Ashmun, L. E., & Brown, R. E. (2013). Post-fire mulching for runoff and erosion mitigation: Part II: Effectiveness in reducing runoff and sediment yields from small catchments. *Catena*, *105*(0), 93-111.

Schröter, K., Llort, X., Velasco-Forero, C., Ostrowski, M., & Sempere-Torres, D. (2011). Implications of radar rainfall estimates uncertainty on distributed hydrological model predictions. *Atmospheric Research*, *100*(2), 237-245.

Sidman, G., Guertin, D. P., Goodrich, D. C., Unkrich, C. L., & Burns, I. S. (2015). Risk assessment of post-wildfire hydrological response in semiarid basins: the effects of varying rainfall representations in the KINEROS2/AGWA model. *International Journal of Wildland Fire* 25(3), 351-362, http://dx.doi.org/10.1071/WF14058

Singh, V. P. (1998). Effect of the direction of storm movement on planar flow. *Hydrological Processes*, *12*(1), 147-170.

Stone, J. J., Lane, L. J., & Shirley, E. D. (1992). Infiltration and runoff simulation on a plane. *Transactions of the ASAE*, *35*(1), 161-170.

Stone, J. J., Paige, G. B., & Hawkins, R. H. (2008). Rainfall intensity-dependent infiltration rates on rangeland rainfall simulator plots. *Transactions of the ASABE*, *51*(1), 45-53.

Unkrich, C. L., Schaffner, M., Kahler, C., Goodrich, D. C., Troch, P., Gupta, H., ... & Yatheendradas, S. (2010). Real-time flash flood forecasting using weather radar and a distributed rainfall-runoff model. In *2nd Joint Federal Interagency Conference, Las Vegas, NV* (p. 11).

Yu, B., Rose, C. W., Coughlan, K. J., & Fentie, B. (1997). Plot-scale rainfall-runoff characteristics and modeling at six sites in Australia and Southeast Asia. *Transactions of the ASAE*, *40*(5), 1295-1303.

U.S. Geological Survey (2013) *National Land Cover Database 2006 Product Legend*. Retrieved from http://www.mrlc.gov/nlcd06_leg.php

U.S. Geological Survey (2014) *The National Map*. Retrieved from http://viewer.nationalmap.gov/basic